学位論文

Extracellular Vesicles from Cancer-Associated Fibroblasts Containing Annexin A6 Induces FAK-YAP Activation by Stabilizing β1 Integrin, Enhancing Drug Resistance
（Cancer associated fibroblasts 由来細胞外小胞中の AnnexinA6 は β1 integrin-FAK-YAP シグナルを介した抗がん剤抵抗性を促進する）

内原　智幸

Tomoyuki Uchihara

熊本大学大学院医学教育部博士課程医学専攻消化器外科学

指導教員

馬場　秀夫　教授

熊本大学大学院医学教育部博士課程医学専攻消化器外科学

2020年3月

学　位　論　文

論文題名　：　**Extracellular Vesicles from Cancer-Associated Fibroblasts Containing Annexin A6 Induces FAK-YAP Activation by Stabilizing β1 Integrin, Enhancing Drug Resistance**
（Cancer associated fibroblasts 由来細胞外小胞中の AnnexinA6 はβ1 integrin-FAK-YAP シグナルを介した抗がん剤抵抗性を促進する）

著 者 名　：　内　原　　智　幸
Tomoyuki Uchihara

指導教員名　：　熊本大学大学院医学教育部博士課程医学専攻消化器外科学　馬場　秀夫　教授

審査委員名　：　消化器内科学担当教授　田中　靖人
細胞医学担当教授　中尾　光善
病態生化学担当教授　山縣　和也
シグナル・代謝医学担当教授　諸石　寿朗

2020年3月

Published OnlineFirst June 30, 2020; DOI: 10.1158/0008-5472.CAN-19-3803

Extracellular Vesicles from Cancer-Associated Fibroblasts Containing Annexin A6 Induces FAK-YAP Activation by Stabilizing β1 Integrin, Enhancing Drug Resistance

Tomoyuki Uchihara[1,2], Keisuke Miyake[1,2], Atsuko Yonemura[1,2], Yoshihiro Komohara[3], Rumi Itoyama[1,2], Mayu Koiwa[1,2], Tadahito Yasuda[1,2], Kota Arima[1,2], Kazuto Harada[1,4], Kojiro Eto[1], Hiromitsu Hayashi[1], Masaaki Iwatsuki[1], Shiro Iwagami[1], Yoshifumi Baba[1], Naoya Yoshida[1], Masakazu Yashiro[5,6], Mari Masuda[7], Jaffer A. Ajani[4], Patrick Tan[8], Hideo Baba[1,9], and Takatsugu Ishimoto[1,2]

ABSTRACT

Extracellular vesicles (EV) from cancer-associated fibroblasts (CAF) are composed of diverse payloads. Although CAFs impact the aggressive characteristics of gastric cancer cells, the contribution of CAF-EV to gastric cancer progression has not been elucidated. Here, we investigated the molecular mechanism of the changes in gastric cancer characteristics induced by CAF-EV. CAF abundance in gastric cancer tissues was associated with poor prognosis of patients with gastric cancer receiving chemotherapy. Moreover, CAF-EV induced tubular network formation and drug resistance of gastric cancer cells in the extracellular matrix (ECM). Comprehensive proteomic analysis of CAF-EV identified that Annexin A6 plays a pivotal role in network formation and drug resistance of gastric cancer cells in the ECM via activation of β1 integrin-focal adhesion kinase (FAK)-YAP. A peritoneal metastasis mouse model revealed that CAF-EV induced drug resistance in peritoneal tumors, and inhibition of FAK or YAP efficiently attenuated gastric cancer drug resistance *in vitro* and *in vivo*. These findings demonstrate that drug resistance is conferred by Annexin A6 in CAF-EV and provide a potential avenue for overcoming gastric cancer drug resistance through the inhibition of FAK-YAP signaling in combination with conventional chemotherapeutics.

Significance: This study elucidates a novel molecular mechanism through which Annexin A6 in CAF-EV activates FAK-YAP by stabilizing β1 integrin at the cell surface of gastric cancer cells and subsequently induces drug resistance.

Graphical Abstract: http://cancerres.aacrjournals.org/content/canres/80/16/3222/F1.large.jpg.

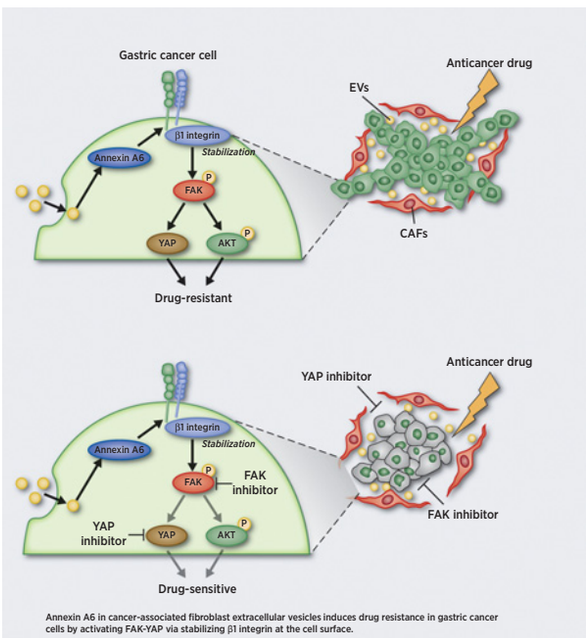

Annexin A6 in cancer-associated fibroblast extracellular vesicles induces drug resistance in gastric cancer cells by activating FAK-YAP via stabilizing β1 integrin at the cell surface.

Introduction

Gastric cancer (GC) is the third leading cause of cancer death worldwide (1), and the treatment strategies for gastric cancer have undergone some modest improvements. For instance, nivolumab, which is an anti-PD-1 immune checkpoint inhibitor, can be used for patients with advanced gastric cancer who exhibit chemoresistance and has been shown to gradually prolong the survival of patients with gastric cancer (2). However, the responses to all gastric cancer treatments are limited,

[1]Department of Gastroenterological Surgery, Graduate School of Medical Sciences, Kumamoto University, Kumamoto, Japan. [2]Gastrointestinal Cancer Biology, International Research Center of Medical Sciences (IRCMS), Kumamoto University, Kumamoto, Japan. [3]Department of Cell Pathology, Kumamoto University, Kumamoto, Japan. [4]Department of Gastrointestinal Medical Oncology, The University of Texas MD Anderson Cancer Center, Houston, Texas. [5]Department of Surgical Oncology, Osaka City University Graduate School of Medicine, Osaka, Japan. [6]Molecular Oncology and Therapeutics, Osaka City University Graduate School of Medicine, Osaka, Japan. [7]Division of Cellular Signaling, National Cancer Center Research Institute, Tokyo, Japan. [8]Program in Cancer and Stem Cell Biology, Duke-NUS Medical School, Singapore. [9]Center for Metabolic Regulation of Healthy Aging, Faculty of Life Sciences, Kumamoto University, Kumamoto, Japan.

Note: Supplementary data for this article are available at Cancer Research Online (http://cancerres.aacrjournals.org/).

Corresponding Authors: Takatsugu Ishimoto, Graduate School of Medical Sciences, Kumamoto University, 1-1-1 Honjo, Kumamoto 860-8556, Japan. Phone: 819-6373-5212; Fax: 819-6371-4378; E-mail: taka1516@kumamoto-u.ac.jp; and Hideo Baba, hdobaba@kumamoto-u.ac.jp

Cancer Res 2020;80:3222–35

doi: 10.1158/0008-5472.CAN-19-3803

Published OnlineFirst June 30, 2020; DOI: 10.1158/0008-5472.CAN-19-3803

and the clinical outcomes of patients with unresectable or recurrent gastric cancer remain far from satisfactory. In particular, the prognosis of patients with gastric cancer with peritoneal metastasis is even worse than that of patients with gastric cancer who do not exhibit peritoneal spread; thus, novel drugs that strengthen the efficiency of the currently available chemotherapies are needed.

The tumor stroma consists of several types of cells—such as T cells, B cells, neutrophils, macrophages, and fibroblasts—that affect tumor progression and drug resistance (3–5). In addition, an accumulating body of evidence shows that a large amount of stroma is associated with poor prognosis in patients with gastric cancer (6–8); thus, the tumor stroma is thought to contain particular molecules that promote tumor progression and drug resistance (9, 10). Cancer-associated fibroblasts (CAF) are found among stromal cells in solid tumors and play a central role in cancer progression, and the molecular mechanisms of CAFs have been extensively investigated (11). Comprehensive genomic and epigenomic analyses of gastric CAFs have demonstrated the role and effects of CAFs on the invasive ability of gastric cancer cells in the extracellular matrix (ECM) through the secretion of factors and direct interactions between CAFs and gastric cancer cells (9, 12, 13). Moreover, recent studies have shown that miRNAs in extracellular vesicles (EV) derived from CAFs (CAF-EV) induce drug resistance in several types of cancer (14, 15). However, CAF-EVs are composed of diverse components other than miRNAs, and the critical factor involved in drug resistance in patients with advanced gastric cancer has not yet been identified.

This study investigated the mechanism through which CAFs impact the sensitivity of gastric cancer cells to chemotherapeutic agents. Here, we show that CAFs elicit characteristic morphologic changes in the ECM and subsequent drug resistance in gastric cancer cells and delineate the molecular mechanism through which Annexin A6 in CAF-EVs induces focal adhesion kinase (FAK)-YAP activation in gastric cancer cells by stabilizing β1 integrin at the cell-ECM interface.

Materials and Methods

Cell lines and cell culture

Human gastric cancer cell lines (AGS, KATO III, MKN45, NUGC3, and NUGC-4) were purchased from the ATCC (AGS), the RIKEN BioResource Center Cell Bank (KATO III, MKN45), and the Japanese Collection of Research Bioresources Cell Bank (NUGC3, NUGC4). CAFs and normal fibroblasts (NF) were established from resected tissues from more than 100 patients with gastric cancer. CAFs were isolated from gastric walls infiltrated by tumors, and NFs were isolated from normal gastric walls. The detailed protocol used to establish these cell lines has been reported previously (12, 16). All the cell lines tested negative for *Mycoplasma* using the e-Myco *Mycoplasma* PCR Detection Kit (catalog no. 25235, Cosmo bio) during the period of this study. These cell lines were cultured in RPMI1640 medium containing 10% FBS and maintained at 37°C in a humidified atmosphere containing 5% CO_2.

qRT-PCR

RNA from cultured cells was extracted using an RNeasy Mini Kit (catalog no. 74106, Qiagen) in accordance with the manufacturer's recommended protocol. mRNA expression was measured by qRT-PCR using TaqMan probes (Roche Diagnostics), and the values were normalized to those of β-actin. All qRT-PCR experiments were conducted with a LightCycler 480 System II (Roche Diagnostics). All qRT-PCR data are shown as the means ± SEs of the mean. The primers used are listed in the Supplementary Table S1.

RNA sequencing

RNA sequencing was conducted as established in a previous study conducted at Kumamoto University (Kumamoto, Japan; ref. 17). RNA sequencing was performed by the Liaison Laboratory Research Promotion Center (Kumamoto University, Kumamoto, Japan) as follows. Total RNA was isolated using the RNeasy Mini Kit (catalog no. 74106, Qiagen), and an Agilent 2100 bioanalyzer (Agilent) was used to measure the total RNA concentration and purity. All the samples with an RNA integrity number >8.0 were used for sequencing. A NextSeq 500 platform (Illumina) was used for the analysis, and the data were converted to Fastq format. The quality of the data was determined by FastQC. The filtered reads were then mapped to the UCSC hg19 reference genome using HISAT2 (v2.1.0). Fragments per kilobase of exon per million mapped reads values were calculated using Cufflinks (v2.2.1). Significant genes ($P < 0.05$) were extracted by Cuffdiff. The RNA sequencing data were deposited in the DDBJ database under the accession number DRA008306.

In vivo chemoresistance assay

Seven-week-old nude BALB/c mice were used for *in vivo* chemoresistance experiments. The mice were injected intraperitoneally with NUGC3 human cells (5×10^6). CAF-EVs (10 μg in 100 μL PBS/mouse), *ANXA6*-depleted CAF-EVs (10 μg in 100 μL PBS/mouse), cisplatin (1.5 mg/kg), and the FAK (15 mg/kg) and YAP inhibitors (50 mg/kg) were also injected intraperitoneally into the mice. The protocol used is described in **Fig. 7A** and **H** and Supplementary Fig. S10. The mice were euthanized 2 days after the final injection, and the intraperitoneal tumors were then removed and weighed. The doses of these inhibitors were based on previous reports (18–20). All animal studies were conducted using protocols approved by Kumamoto University Institutional Animal Care and Use Committee.

Human samples

Primary gastric cancer tissues were obtained from 335 patients with gastric cancer at pathologic stage I, II, III, or IV who underwent definitive gastrectomy and received chemotherapy before/after palliative surgery or biopsy at Kumamoto University Hospital from April 2005 to December 2016. Primary CAFs were established from patients with gastric cancer who underwent gastrectomy at Kumamoto University Hospital and Saiseikai Kumamoto Hospital from 2013 to 2019.

Study approval

This research was approved by the Medical Ethics Committee of Kumamoto University (Kumamoto, Japan) and Saiseikai Kumamoto Hospital. Written informed consent to participate in this study was obtained from all the patients.

Statistical analysis

All the experiments were performed in triplicate, and the data shown are representative of consistent results. The data are presented as the means ± SEs of the means. The Mann–Whitney *U* test was used to compare continuous variables between two groups. Categorical variables were compared using the χ^2 test. Kaplan–Meier curves and the generalized Wilcoxon test were used to evaluate the statistical significance of the differences. For the statistical analyses, we used JMP (version 9, SAS Institute) and SAS software (version 9.1, SAS Institute) with the assumptions required for the respective tests. Statistical significance was indicated if the *P* values were lower than 0.05, and all the data met the assumptions regarding distribution and variance in the statistical test used.

Results

CAFs enhance the tubular network formation and subsequent drug resistance of gastric cancer cells in the ECM

To quantify the amount of CAFs in gastric cancer tissues, resected tissues from 335 patients with gastric cancer were subjected do IHC

Published OnlineFirst June 30, 2020; DOI: 10.1158/0008-5472.CAN-19-3803

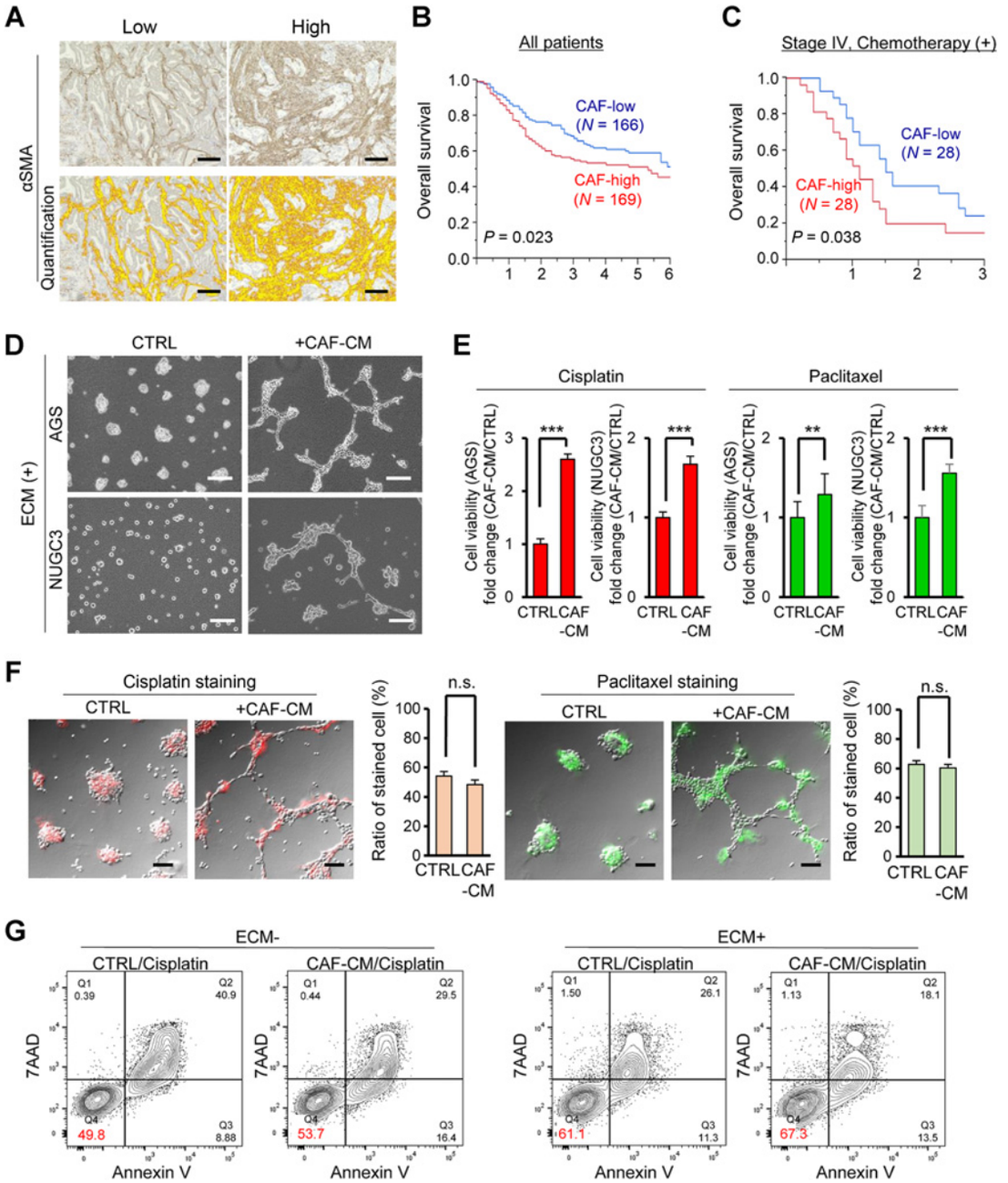

Figure 1.

CAFs promote the tubular network formation and subsequent drug resistance of gastric cancer cells in the ECM. **A,** Representative IHC staining of αSMA and quantification of αSMA-positive cells. Scale bars, 200 μm. **B,** Overall survival curves of all patients with gastric cancer based on their αSMA status. **C,** Overall survival curves of patients with stage IV gastric cancer treated with chemotherapy based on their αSMA status. **D,** Morphology of gastric cancer cells (AGS and NUGC3) cultured with normal medium (CTRL)/CAF-CM in ECM-coated plates. Scale bars, 200 μm. **E,** Viability of gastric cancer cells treated with cisplatin or paclitaxel for 24 hours and then cultured with normal medium (CTRL)/CAF-CM in ECM-coated plates. **F,** Representative image showing the incorporation of fluorophore-conjugated cisplatin and paclitaxel in gastric cancer cells in the ECM. The column graph shows the quantification of stained cells. Scale bars, 100 μm. **G,** Apoptosis assay of gastric cancer cells treated with cisplatin for 24 hours and then cultured with normal medium (CTRL) or CAF-CM in the ECM. The cells were stained with Annexin V and 7-aminoactinomycin D (7-AAD). n.s., not significant; **, $P < 0.01$; ***, $P < 0.001$.

staining using an antibody specific for alpha-smooth muscle actin (αSMA). According to the proportion of αSMA-positive stroma, the patients were divided into the CAF-low or CAF-high groups (**Fig. 1A**). We subsequently assessed the relationship between gastric cancer patient survival and the amount of CAFs by Kaplan–Meier analysis. Patients with gastric cancer harboring CAF-high tumors exhibited significantly shorter overall survival ($P = 0.023$; **Fig. 1B**). Moreover, patients with stage IV gastric cancer with CAF-high tumors who

Published OnlineFirst June 30, 2020; DOI: 10.1158/0008-5472.CAN-19-3803

received chemotherapy had remarkably shorter overall survival ($P = 0.038$; **Fig. 1C**).

On the basis of these results, we first hypothesized that CAFs in the tumor stroma are involved in mediating the drug resistance of gastric cancer cells. To test this hypothesis, the sensitivity to cisplatin and paclitaxel was examined in AGS and NUGC3 cells treated with conditioned medium (CM) from CAFs (CAF-CM). AGS and NUGC3 cells treated with CAF-CM on normal culture plates showed no morphologic changes, and neither cell line exhibited resistance to cisplatin or paclitaxel (Supplementary Fig. S1A and S1B). However, gastric cancer cells treated with CAF-CM exhibited tubular network formation within a few hours of culture on plates coated with Matrigel (**Fig. 1D**; Supplementary movies S1 and S2). Tubular network formation is thought to be associated with the invasive characteristics of cancer cells (21, 22). Notably, gastric cancer cells forming tubular networks in the ECM exhibited marked resistance to cisplatin and paclitaxel (**Fig. 1E**). However, AGS and NUGC3 cells treated with GC-CM did not show morphologic changes in the ECM or resistance to cisplatin and paclitaxel (Supplementary Fig. S1C and S1D).

To address the mechanism of drug resistance in gastric cancer cells treated with CAF-CM, the incorporation of fluorescence-conjugated cisplatin and paclitaxel into gastric cancer cells in the ECM was tested. No difference in cisplatin and paclitaxel incorporation was found between untreated gastric cancer cells and gastric cancer cells treated with CAF-CM (**Fig. 1F**). We then predicted that gastric cancer cells in the ECM treated with CAF-CM would exhibit slow cycling according to a cell-cycle analysis because anticancer drugs such as cisplatin and paclitaxel mainly target rapidly proliferating cancer cells (23). However, the results from a cell-cycle analysis revealed that the proportion of proliferating gastric cancer cells in the ECM treated with CAF-CM was higher than that in the control group (Supplementary Fig. S2A). Moreover, we examined apoptosis in gastric cancer cells treated with or without CAF-CM after cisplatin treatment. Notably, among all the groups, the highest proportion of viable gastric cancer cells in the ECM was detected after treatment with CAF-CM (**Fig. 1G**). A Western blotting analysis also revealed gastric cancer cells treated with CAF-CM in the ECM exhibited increased Bcl-2 expression and decreased cleaved caspase-3 and cleaved PARP expression (Supplementary Fig. S2B). These results indicate that the apoptosis of CAF-CM–treated gastric cancer cells in the ECM is inhibited through the activation of antiapoptotic signaling.

EVs in CAF-CM strongly induce tubular network formation and drug resistance in gastric cancer cells in the ECM

Because gastric cancer cells treated with CAF-CM acquire drug resistance in the ECM, we conducted RNA sequencing to identify unique molecular patterns in gastric cancer cells in the ECM 3 and 24 hours after CAF-CM treatment and compared these patterns with those in gastric cancer cells without CAF-CM treatment. We found that 944, 516, and 657 genes were differentially expressed after 3 hours, after 24 hours, and after both 3 and 24 hours compared with their expression in the control group (Supplementary Fig. S3A–S3D). Moreover, a gene ontology (GO) analysis of the 2,117 differentially expressed genes revealed the particular upregulation of ECM-related and plasma membrane–related genes (**Fig. 2A**). A network analysis confirmed the activation of the ECM and integrin-binding signaling (**Fig. 2B**). On the basis of the results from these analyses and previous findings that EVs affect the surface receptors in target cells (24), we presumed that CAF-EVs might be involved in network formation and drug resistance. Thus, we extracted CAF-EVs by ultracentrifugation, and AGS and NUGC3 cells were treated with CAF-CM, CAF-EVs, or CAF-CM supernatant (**Fig. 2C** and **D**). Notably, gastric cancer cells treated with CAF-EVs exhibited network formation and cisplatin resistance, whereas AGS and NUGC3 cells treated with EV-depleted CAF-CM supernatant exhibited almost no network formation (**Fig. 2E**, **F**, and **K**). In addition, we blocked the secretion of CAF-EVs by GW4869 treatment, and the AGS and NUGC3 cells treated with CAF-EVs from GW4869-treated CAFs exhibited almost no network formation (**Fig. 2G–J**). These findings suggest that EVs contained in CAF-CM play a central role in network formation and drug resistance in gastric cancer cells.

Annexin A6 in CAF-EVs has important functions in tubular network formation and drug resistance

EVs are composed of membrane proteins, intracellular proteins, miRNAs, and DNAs and transport these factors to other cells (25). The EVs used in our experiments were characterized by transmission electron microscopy, nanoparticle tracking analysis, and Western blotting analysis of conventional EV markers, in accordance to previous studies (Supplementary Fig. S4A–S4C; refs. 26, 27). Because the network formation of gastric cancer cells in the ECM was rapidly induced within 3 hours of treatment with CAF-EVs, we hypothesized that certain proteins play a role in this phenomenon. Thus, we conducted a comprehensive proteomic analysis using GC-EVs or CAF-EVs and identified proteins that are highly expressed in CAF-EVs but not GC-EVs (**Fig. 3A**). We then conducted a loss-of-function study using *ANXA6, CD44, COL12A1,* or *TUBA1A* siRNA to identify a potential mediator involved in the network formation of gastric cancer cells in the ECM (Supplementary Fig. S5A–S5D). We demonstrated that the network formation of gastric cancer cells was not affected by *CD44*-, *COL12A1*-, or *TUBA1A*-depleted EVs (Supplementary Fig. S5E). We further silenced *ANXA6* in CAFs using two siRNAs and treated AGS and NUGC3 cells with EVs isolated from control siRNA- or *ANXA6* siRNA-transfected CAFs. Strikingly, *ANXA6*-depleted EVs diminished both the network formation and cisplatin resistance of gastric cancer cells in the ECM (**Fig. 3B–D**; Supplementary Fig. S5E), although no difference in the number of EVs isolated from CAFs transfected with control siRNA and the *ANXA6* siRNAs was found (**Fig. 3E**). Similar to its expression in isolated CAFs, Annexin A6 was specifically expressed in αSMA-positive CAFs in the tumor stroma of human gastric cancer tissue (**Fig. 3F**). These findings suggest that Annexin A6 in CAF-EVs plays a critical role in the network formation and drug resistance in gastric cancer cells in the ECM and that its functional role is active in both gastric cancer tissues and isolated CAFs.

Annexin A6 in CAF-EVs is transferred into gastric cancer cells, where it stabilizes β1 integrin at the gastric cancer cell surface

According to the results from the network analysis of the RNA sequencing data, integrin-binding signaling was activated in gastric cancer cells in the ECM treated with CAF-CM. Integrins comprise a large family of heterodimeric cell surface receptors that play a central role in the interactions between cells and the ECM (28). In addition, the β1 integrin subunit can bind to 12 different integrin α chains of the integrin family (29) and has been shown to play important roles in a variety of cells in the tumor microenvironment (30) and in mediating

Published OnlineFirst June 30, 2020; DOI: 10.1158/0008-5472.CAN-19-3803

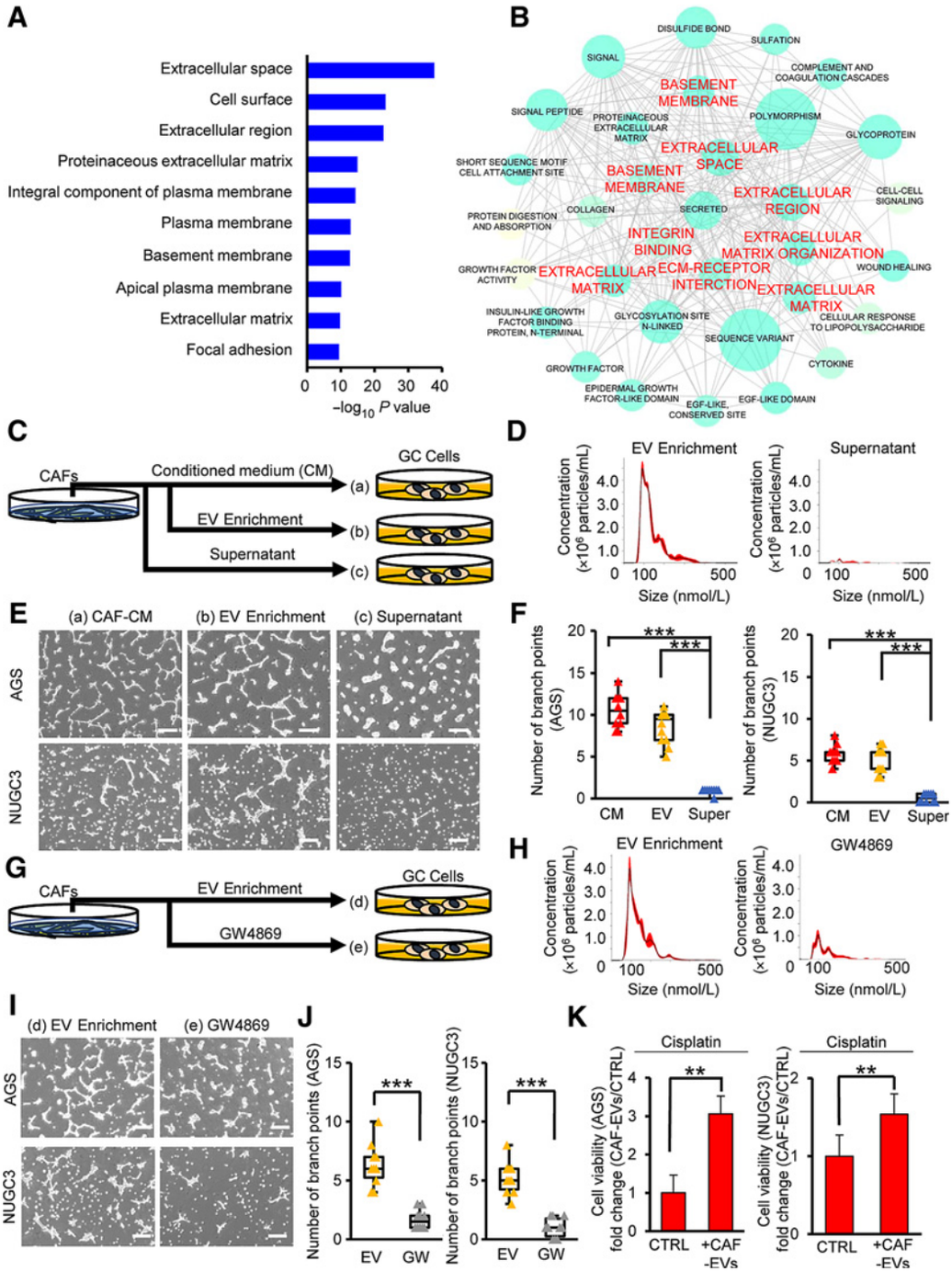

Figure 2.

CAF-EVs induce tubular network formation and drug resistance in gastric cancer cells in the ECM. **A** and **B,** Integrated analysis of upregulated and downregulated genes. These genes were identified from the RNA sequencing data as genes that were upregulated and downregulated by 2.0-fold in gastric cancer cells after 3 and 24 hours of CAF-CM treatment. Top GO terms associated with cellular component (**A**) and network analysis (**B**) identified from RNA sequencing data of gastric cancer cells after 3 and 24 hours of CAF-CM treatment. **C,** Protocol for evaluating the network formation of gastric cancer cells in the ECM after treatment with CAF-CM (a), enrichment of CAF-EVs by ultracentrifugation (b), and collection of CM supernatant after CAF-EV enrichment (c). **D,** Numbers and size distributions of CAF-EVs and the supernatant obtained using NanoSight. **E** and **F,** Morphology (**E**) and quantification (**F**) of network formation of gastric cancer cells after the treatments detailed in a, b, and c. Scale bars, 500 μm. **G,** Protocol used for evaluating the network formation of gastric cancer cells in the ECM after treatment with CAF-EVs (d) and GW4869-treated CAF-EVs (e). **H,** Numbers and size distributions of CAF-EVs and the supernatant obtained using NanoSight. **I** and **J,** Morphology (**I**) and quantification (**J**) of the network formation of gastric cancer cells after the treatments detailed in d and e. Scale bars, 500 μm. **K,** Viability of gastric cancer cells treated with cisplatin for 24 hours and then cultured with normal medium (CTRL) or CAF-EVs. **, $P < 0.01$; ***, $P < 0.001$.

Published OnlineFirst June 30, 2020; DOI: 10.1158/0008-5472.CAN-19-3803

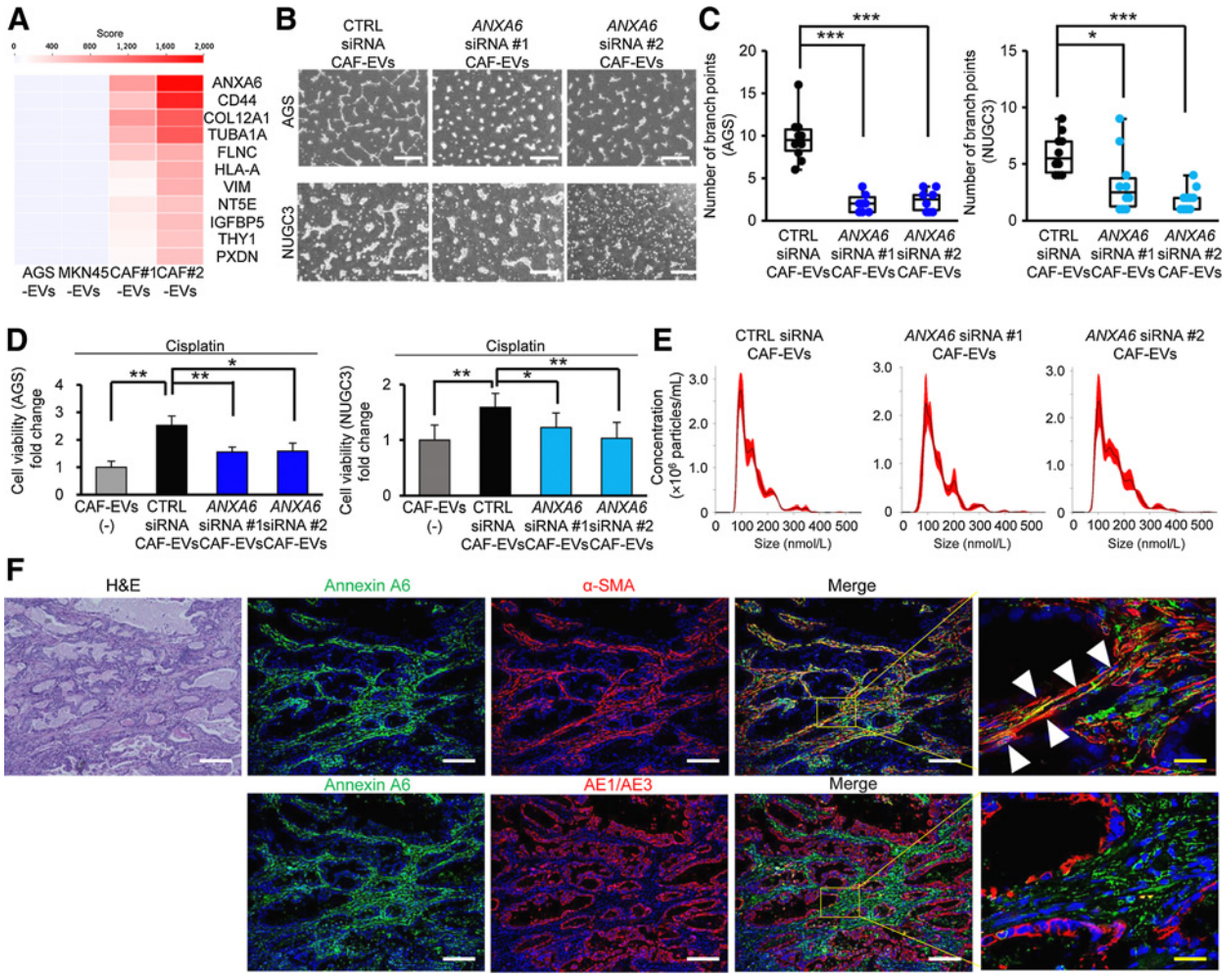

Figure 3.

Annexin A6 in CAF-EVs is involved in tubular network formation and drug resistance. **A,** Heatmap showing specific proteins expressed at higher levels in CAF-EVs than in GC-EVs. **B–D,** Morphology (**B**), network formation (**C**), and viability (**D**) of gastric cancer cells after treatment with CAF-EVs transfected with *ANXA6* siRNAs (#1 or #2) relative to that obtained after treatment with CAFs transfected with control siRNA. Scale bars, 500 μm. **E,** Numbers and size distributions of CAF-EVs transfected with *ANXA6* siRNAs (#1 or #2) and control siRNA determined using NanoSight. **F,** Representative hematoxylin and eosin (H&E) and immunofluorescence staining for Annexin A6 and αSMA, respectively; the nucleus was stained with DAPI (top). The merging of Annexin A6 and AE1/AE3 staining with DAPI nuclear staining is shown in the bottom panel. Scale bars: white, 200 μm; yellow, 30 μm. *, $P < 0.05$, **, $P < 0.01$; ***, $P < 0.001$.

the invasion and migration of gastric cancer cells (12). We therefore focused on β1 integrin and first examined the expression of β1 integrin and Annexin A6 in gastric cancer cells and CAFs. Western blotting analysis revealed that β1 integrin is expressed at a higher level in CAFs than in gastric cancer cells and that Annexin A6 is specifically expressed in CAFs but not gastric cancer cells (**Fig. 4A**). Subsequently, we examined *ITGB1* mRNA expression and β1 integrin protein expression in three experimental replicates of AGS cells treated with CAF-EVs by qRT-PCR and Western blotting analysis, respectively. Although no differences in *ITGB1* mRNA expression was found between the control and CAF-EVs groups (**Fig. 4B**), β1 integrin protein expression was markedly higher in the AGS and NUGC3 cells treated with CAF-EVs (**Fig. 4C**; Supplementary Fig. S6A). Moreover, we extracted cell membrane proteins and showed that CAF-EV treatment significantly increased the expression of β1 integrin at the surface of AGS cells (**Fig. 4D**). However, there is still a possibility that newly synthesized and trafficking pools of β1 integrin are contained in the extracted plasma membrane proteins. Because cell surface β1 integrin is determined by the amount of the integrin α subunit (30), we examined the expression of integrin α subunits and showed that the expression of integrin α1, 2, 3, 6, and 7 was significantly increased in AGS cells treated with CAF-EVs in the ECM (Supplementary Fig. S6B). We also examined the expression of β1 integrin and Annexin A6 in AGS cells treated with CAF-EVs in the ECM by immunofluorescence analysis and found that the expression of β1 integrin at the surface was markedly increased in Annexin A6–incorporated AGS cells after CAF-EV treatment compared with their expression in control medium (**Fig. 4E**). Although there is a possibility that cytoplasmic expression of β1 integrin shows the localization in endosomes, we confirmed the colocalization of β1 integrin and EpCAM as a cell surface marker that strengthens β1 integrin stabilization at the cell surface (**Fig. 4F**).

Published OnlineFirst June 30, 2020; DOI: 10.1158/0008-5472.CAN-19-3803

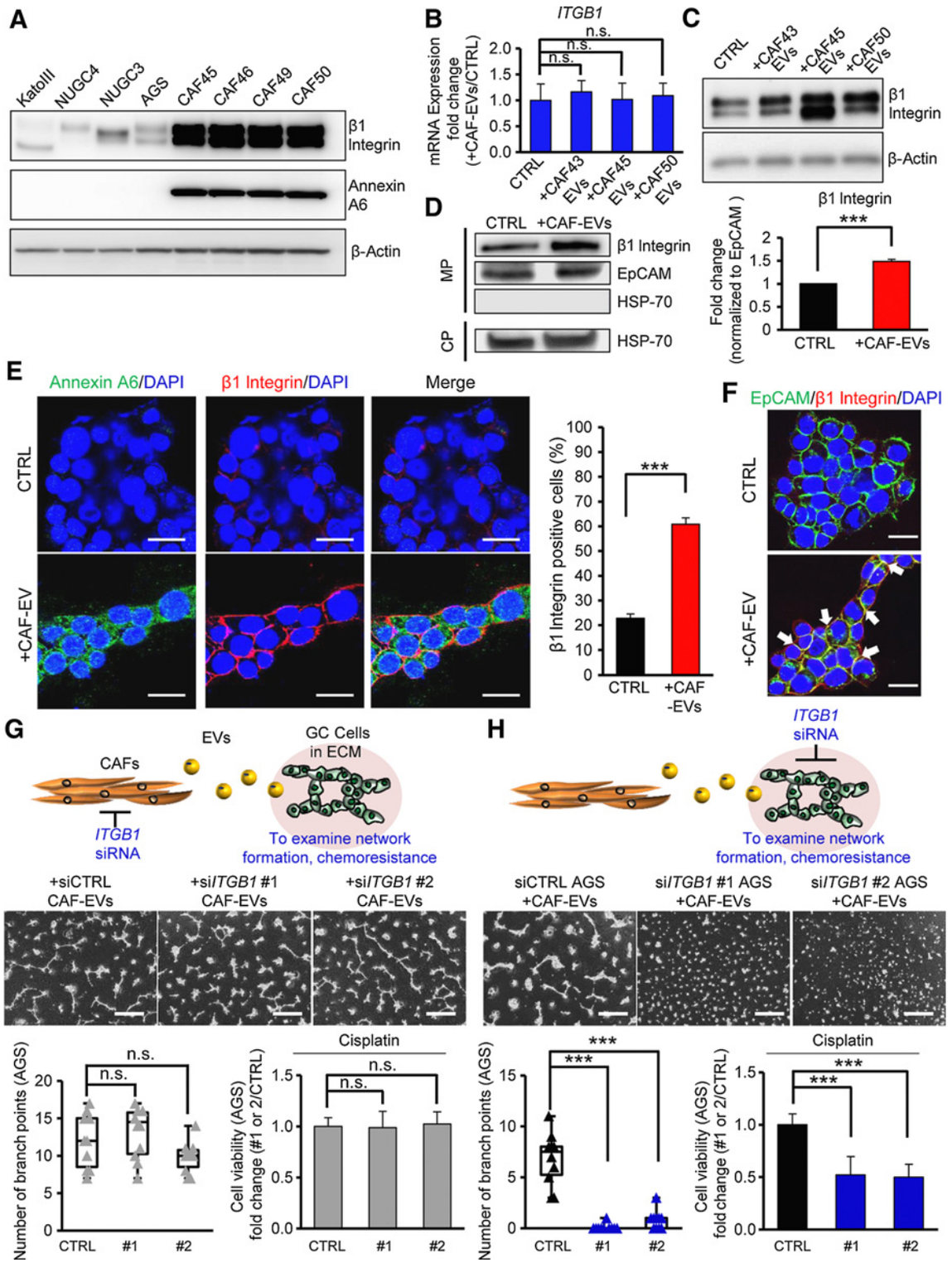

Figure 4.

Annexin A6 in CAF-EVs is taken up by gastric cancer cells, where it stabilizes β1 integrin at the gastric cancer cell surface. **A,** The expression of β1 integrin and Annexin A6 in gastric cancer cell lines (AGS) and CAFs was evaluated by Western blotting analysis. **B** and **C,** The *ITGB1* and β1 integrin expression levels in a gastric cancer cell line treated with CAF-EVs were determined by qRT-PCR (**B**) and Western blotting analysis (**C**). **D,** Expression levels and quantification of β1 integrin, EpCAM, and HSP70 among the extracted plasma membrane proteins (MP) and cytosolic proteins (CP) from gastric cancer cells after culture with normal medium (CTRL) or CAF-EVs. (*Continued on the following page.*)

Published OnlineFirst June 30, 2020; DOI: 10.1158/0008-5472.CAN-19-3803

Plasma membrane proteins expressed on EVs are transferred to target cells through membrane fusion (24). On the basis of this evidence, we investigated two possibilities, namely, that β1 integrin on CAF-EVs is transferred into gastric cancer cells via membrane fusion between CAF-EVs and gastric cancer cells and that β1 integrin at the cell surface of gastric cancer cells is stabilized via CAF-EV incorporation into gastric cancer cells. To investigate these hypotheses, we silenced *ITGB1* in CAFs or AGS cells using two siRNAs (Supplementary Fig. S7A and S7B), and AGS cells were treated with EVs. Although EVs from *ITGB1*-silenced CAFs did not decrease the network formation and cisplatin resistance of gastric cancer cells in the ECM (**Fig. 4G**), *ITGB1*-silenced gastric cancer cells treated with CAF-EVs exhibited both decreased network formation and cisplatin resistance in the ECM (**Fig. 4H**). These results suggest that the CAF-EV–induced increase in cell surface β1 integrin expression in gastric cancer cells is critical for gastric cancer cell network formation and drug resistance in the ECM.

Annexin A6 stabilizes β1 integrin at the gastric cancer cell surface and subsequently enhances drug resistance

Annexin A6 and β1 integrin have been found to be important in gastric cancer cell network formation in the ECM; thus, we predicted that Annexin A6 and β1 integrin interact with one another. We first examined *ITGB1* mRNA expression and protein expression in *ANXA6*-silenced CAFs. Although no differences in *ITGB1* mRNA expression was found between CAFs transfected with control siRNA and those transfected with the *ANXA6* siRNAs (Supplementary Fig. S8), β1 integrin protein expression was markedly lower in CAFs transfected with the *ANXA6* siRNAs than in CAFs transfected with control siRNA (**Fig. 5A**). In contrast, Annexin A6 protein expression in CAFs transfected with *ITGB1* siRNAs was not affected (**Fig. 5B**). Moreover, we performed a protein stability assay using the protein synthesis inhibitor cycloheximide (CHX) to investigate the effect of Annexin A6 expression on the levels of β1 integrin in CAFs. After treatment with CHX, the levels of β1 integrin in CAFs transfected with *ANXA6* siRNAs exhibited more rapid and significant decreases compared with the levels in CAFs transfected with control siRNA (**Fig. 5C**). Furthermore, flow cytometry and immunofluorescence analyses revealed that the cell surface expression of β1 integrin was lower in gastric cancer cells treated with *ANXA6*-depleted EVs (**Fig. 5D** and **E**). In contrast, to determine whether increased Annexin A6 expression affects cell surface β1 integrin expression, network formation, and drug resistance, we constructed an *ANXA6* expression vector and confirmed the expression of Annexin A6 in AGS cells with either the control or *ANXA6* vector (**Fig. 5F**). Flow cytometry and immunofluorescence analyses revealed the recovery of β1 integrin expression on the surface of *ANXA6*-overexpressing AGS cells treated with *ANXA6*-depleted EVs (**Fig. 5G–I**). In addition, *ANXA6*-overexpressing AGS cells regained their network formation and drug resistance capabilities following treatment with *ANXA6*-depleted EVs (**Fig. 5G**, **J**, and **K**). These findings strongly support the notion that β1 integrin expression at the surface of gastric cancer cells in the ECM is enhanced by Annexin A6 in CAF-EVs.

Integrin-FAK signaling plays critical roles in tubular network formation in the ECM and drug resistance in gastric cancer cells treated with CAF-EVs

FAK, a cytoplasmic tyrosine kinase, is a key mediator of intracellular signaling upon the integrin-mediated adhesion of cells to the ECM and is an upstream regulator of PI3K-AKT signaling that transduces an β1 integrin viability signal in the ECM (31). Moreover, emerging evidence shows that the Hippo pathway is a potent mediator of integrin signaling (32, 33). Because signaling pathways downstream of integrin are regulated by protein–protein interactions, we further performed a comprehensive proteomic analysis of gastric cancer cells treated with and without CAF-CM as well as RNA sequencing. Differentially expressed genes related to focal adhesion and the PI3K-AKT and Hippo signaling pathways were identified in gastric cancer cells treated with CAF-CM according to a pathway analysis of the comprehensive transcriptomics and proteomics data (**Fig. 6A**). A Western blotting analysis revealed that the phosphorylation of FAK and AKT and the level of YAP were increased in AGS cells treated with CAF-EVs compared with those in untreated cells (**Fig. 6B**), and an immunofluorescence analysis showed the nuclear translocation of YAP in AGS cells treated with CAF-EVs (Supplementary Fig. S9). Moreover, the activation of this signaling pathway by CAF-EVs was attenuated in AGS cells treated with *ANXA6*-depleted EVs (**Fig. 6C**). We subsequently used respective inhibitors and found that the activation was effectively blocked by an FAK inhibitor (**Fig. 6D–F**). Notably, CAF-EVs induced network formation and subsequent cisplatin resistance of AGS cells in the ECM, and these effects were strongly attenuated by the FAK inhibitor (**Fig. 6G** and **H**). Similarly, the YAP inhibitor verteporfin markedly reduced the network formation and drug resistance of AGS cells treated with CAF-EVs (**Fig. 6I** and **J**), whereas an AKT inhibitor slightly attenuated these phenomena (**Fig. 6K** and **L**). These findings indicate that integrin-FAK signaling and subsequent YAP activation play a critical role in network formation in the ECM and drug resistance of gastric cancer cells treated with CAF-EVs.

FAK and YAP inhibitors markedly attenuate drug resistance enhanced by CAF-EVs in a peritoneal metastasis mouse model

To verify the significance of CAF-EVs in gastric cancer drug resistance in an *in vivo* model, NUGC3 cells were injected into the peritoneal cavities of nude mice. The mice were subsequently treated with PBS, cisplatin, CAF-EVs, or cisplatin plus CAF-EVs according to the protocol shown in **Fig. 7A**. Cisplatin treatment significantly reduced the growth of peritoneal tumors, whereas treatment with cisplatin plus CAF-EVs did not exert an antitumor effect (**Fig. 7B** and **C**), which suggests that CAF-EVs play a role in the drug resistance of gastric cancer cells *in vivo* as well as *in vitro*. Moreover, TUNEL revealed significantly fewer apoptotic tumor cells in mice treated with

(*Continued.*) **E,** Immunofluorescence staining for β1 integrin and Annexin A6 and DAPI nuclear staining in gastric cancer cells (top) and gastric cancer cells treated with CAF-EVs (bottom). The column graph shows the quantification of cell surface β1 integrin-positive gastric cancer cells. Scale bars, 20 μm. **F,** Immunofluorescence staining for β1 integrin and EpCAM and DAPI nuclear staining in gastric cancer cells (top) and gastric cancer cells treated with CAF-EVs (bottom). The arrows highlight the colocalization between β1 integrin and EpCAM at the cell surface. Scale bars, 20 μm. **G,** Protocol, morphology, and quantification of network formation and viability of gastric cancer cells after treatment with CAF-EVs transfected with *ITGB1* siRNAs (#1 or #2) relative to those found after treatment with CAFs transfected with control siRNA. Scale bars, 500 μm. **H,** Protocol, morphology, and quantification of the network formation and viability of gastric cancer cells transfected with *ITGB1* siRNAs (#1 or #2) and treated with CAF-EVs relative to those of gastric cancer cells transfected with control siRNA. Scale bars, 500 μm. n.s., not significant; *, $P < 0.05$, ***, $P < 0.001$.

Published OnlineFirst June 30, 2020; DOI: 10.1158/0008-5472.CAN-19-3803

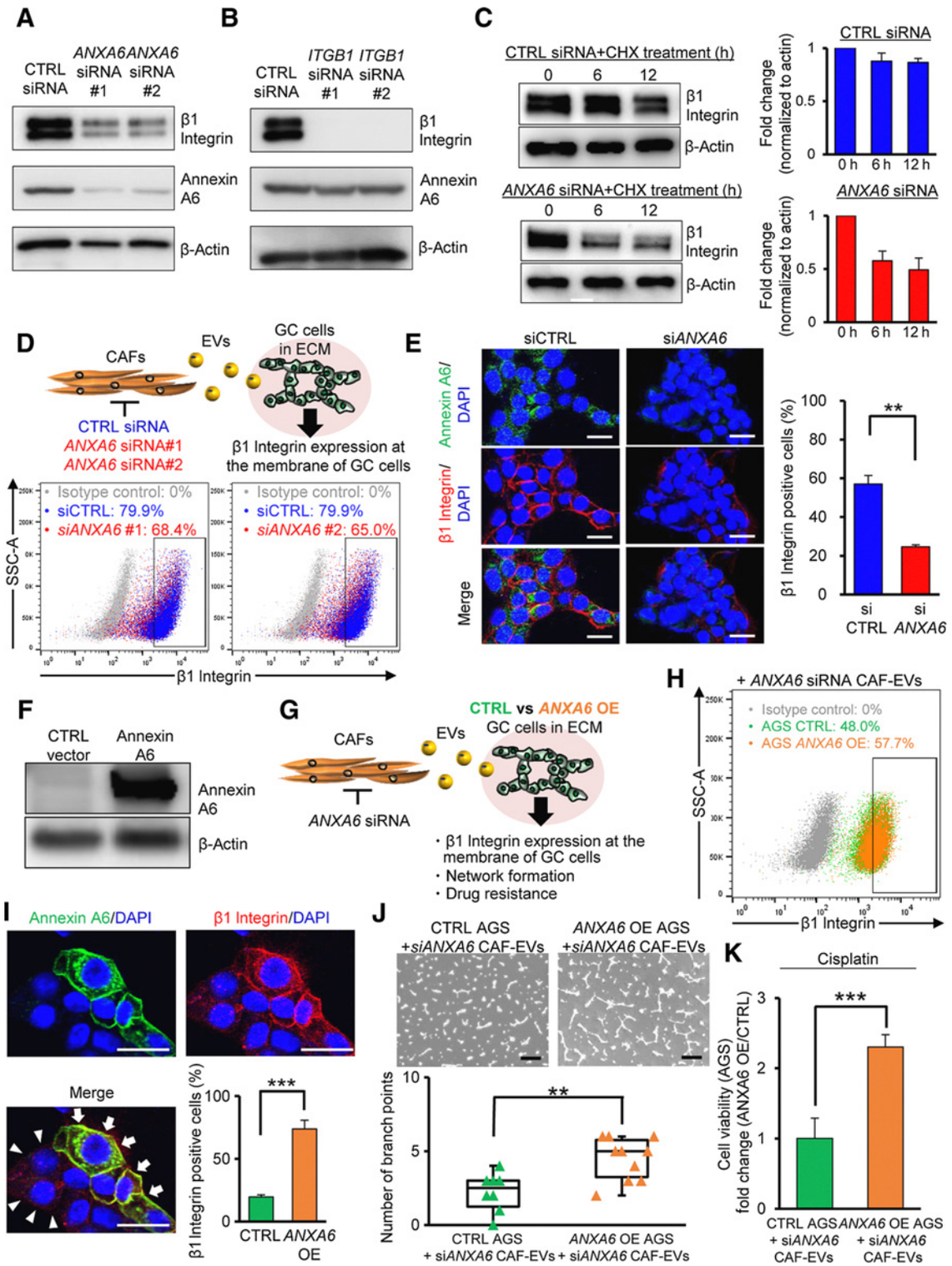

Figure 5.

Annexin A6 stabilizes β1 integrin at the gastric cancer cell surface and enhances drug resistance. **A,** The expression of β1 integrin and Annexin A6 in CAFs transfected with *ANXA6* siRNAs (#1 or #2) relative to that in CAFs transfected with control siRNA was evaluated by Western blotting analysis. **B,** The expression of β1 integrin and Annexin A6 in CAFs transfected with *ITGB1* siRNAs (#1 or #2) relative to that in CAFs transfected with control siRNA was evaluated by Western blotting analysis. **C,** The left panels show an immunoblot analysis of β1 integrin and β-actin in CAFs stably expressing control or Annexin A6 siRNAs and exposed to CHX (40 μg/mL) for the indicated times. (*Continued on the following page.*)

Published OnlineFirst June 30, 2020; DOI: 10.1158/0008-5472.CAN-19-3803

cisplatin plus CAF-EVs than in those treated with only cisplatin (**Fig. 7D** and **E**). Importantly, cisplatin treatment significantly reduced the growth of peritoneal tumors in mice treated with *ANXA6*-depleted EVs compared with those belonging to the control siRNA group (**Fig. 7F** and **G**; Supplementary Fig. S10). These results indicate the significance of Annexin A6 in CAF-EVs for the induction of drug resistance *in vivo*.

We then examined whether FAK and YAP inhibitors could attenuate the cisplatin resistance of gastric cancer cells mediated by CAF-EVs. The antitumor effect of cisplatin was recovered by additional treatment with the FAK and YAP inhibitors, which suggests that the FAK-YAP signaling pathway plays a critical role in the drug resistance of peritoneal tumors enhanced by CAF-EVs (**Fig. 7H** and **I**).

Discussion

Patients with gastric cancer with a high stromal content, as determined by either gene expression analysis or histopathologic evaluation, exhibit poor prognoses (34). CAFs are a major component of the tumor stroma and secrete various soluble factors that have been associated with tumor progression and drug resistance (11). In accordance with the results from previous studies, CAF-high tumors were significantly correlated with poor gastric cancer patient prognosis. Moreover, patients with stage IV gastric cancer with CAF-high tumors who received chemotherapy also exhibited markedly poor prognoses. Here, we provide molecular evidence demonstrating that a large number of CAFs leads to poor gastric cancer patient prognosis by enhancing drug resistance. Gastric cancer cells in the ECM treated with CAF-EVs exhibited network formation due to β1 integrin stabilization and subsequent drug resistance, and CAF-EVs enhanced the drug resistance of gastric cancer cells in a peritoneal metastasis mouse model.

The communication between cancer cells and the stroma is facilitated by EVs (35–37). EVs, which have a diameter of 100–1,000 nm, are formed and released by budding from the plasma membranes of several types of cells (38). These vesicles expose membrane proteins at their surface and contain various types of cytosolic proteins and biomolecules (25). Because CAF-EVs were found to induce rapid morphologic changes in gastric cancer cells in the ECM in this study, we conducted a comprehensive proteomic analysis using isolated EVs and identified Annexin A6 as a specific protein in CAF-EVs. Annexin A6, a member of a conserved superfamily of Ca^{2+}-dependent phospholipid-binding proteins, is highly expressed and a potential prognostic marker in several types of malignancies, such as acute lymphoblastic leukemia and cervical cancer (39, 40). Moreover, the roles of Annexin A6 in cancer cell migration have been investigated, and multiple scaffolding functions have been identified (41, 42). In contrast, the expression of Annexin A6, which modulates EGFR signaling, is often downregulated in various types of cancers (43, 44). Because the available evidence regarding the functional role of Annexin A6 is based on experiments using cancer cells, the significance of Annexin A6 in the tumor microenvironment remains unknown. A recent study provided compelling evidence showing that Annexin A6-positive EVs support pancreatic ductal adenocarcinoma aggressiveness through the Annexin A6/low density lipoprotein receptor–related protein 1/thrombospondin1 complex and that Annexin A6–positive EVs in serum are a potential biomarker for the pancreatic ductal adenocarcinoma grade (27). In addition, we demonstrated that Annexin A6 in CAF-EVs stabilizes β1 integrin expression at the cell surface of gastric cancer cells in the ECM, which results in drug resistance in gastric cancer cells through the activation of FAK-YAP signaling. In contrast, another annexin family member, Annexin A2, enhances the internalization of cell surface β1 integrin in intestinal epithelial cells (45). Our present findings provide a rationale for the cancer-promoting function of Annexin A6 carried by CAF-EVs from the tumor microenvironment and identify the FAK-YAP signaling pathway as a critical intracellular signaling pathway for the drug resistance of gastric cancer cells in the ECM.

The Hippo pathway controls the organ size in a diverse group of species, and Hippo pathway deregulation can induce tumors in model organisms and is observed in a wide range of human carcinomas, including lung, colorectal, ovarian, and liver cancer (46). In addition, various components of the Hippo pathway, such as TAZ and YAP, are involved in drug resistance during cancer treatment (47). A bioinformatic analysis of uveal melanoma revealed that FAK regulates YAP activation through MOB1 phosphorylation and that FAK inhibition represses the transcriptional activity of YAP (48). Furthermore, we found that β1 integrin on the surface of gastric cancer cells was stabilized by Annexin A6 in CAF-EVs and observed subsequent FAK-YAP activation in gastric cancer cells in the ECM treated with CAF-EVs. These findings suggest that outside-in signaling activated by the binding of integrins to the ECM is activated by Annexin A6 in CAF-EVs and that this activation leads to FAK-YAP activation and the induction of drug resistance in gastric cancer cells in the ECM.

In conclusion, Annexin A6 in EVs derived from CAFs stabilizes β1 integrin at the plasma membrane of gastric cancer cells in the ECM. Subsequently, phosphorylated FAK leads to AKT activation and YAP accumulation, which results in the network formation of gastric cancer cells in the ECM and their substantial drug resistance (**Fig. 7J**). Moreover, blockade by an FAK or a YAP inhibitor but not an AKT inhibitor effectively inhibited the drug resistance of gastric cancer cells. The findings of this study provide evidence demonstrating that FAK-YAP signaling activated by Annexin A6 in CAF-EVs from the tumor

(*Continued.*) In the right panels, the mean values ± SDs from three independent experiments for the β1 integrin-to-β-actin band intensity ratio relative to the corresponding value at time zero (0) are shown. **D,** The expression of β1 integrin at the gastric cancer cell membrane after treatment with CAF-EVs transfected with *ANXA6* siRNAs relative to that after treatment with CAFs transfected with control siRNA was determined by flow cytometry. **E,** Immunofluorescence staining for β1 integrin and Annexin A6 and DAPI nuclear staining in gastric cancer cells after treatment with CAF-EVs transfected with control siRNA (top) and *ANXA6* siRNAs (bottom). The column graph shows the quantification of cell surface β1 integrin-positive cells. Scale bars, 20 μm. **F,** Immunoblot analysis of Annexin A6 in gastric cancer cells transfected with control vector and an *ANXA6* overexpression vector. The expression of β-actin was similarly analyzed as a loading control. **G,** Experimental protocol. **H,** β1 integrin expression at the gastric cancer cell membrane was determined by flow cytometry. Immunofluorescence staining for β1 integrin and Annexin A6 combined with DAPI staining. Arrows, cell surface β1 integrin–positive cells; arrowheads, cell surface β1 integrin-negative cells. Scale bars, 10 μm. **I** and **J,** Morphology (**I**) and quantification of network formation (**J**). Scale bars, 500 μm (**J**). **K,** Gastric cancer cell viability after treatment with CAF-EVs transfected with *ANXA6* siRNAs relative to that after treatment with CAFs transfected with control siRNA. n.s., not significant; **, $P < 0.01$; ***, $P < 0.001$.

Published OnlineFirst June 30, 2020; DOI: 10.1158/0008-5472.CAN-19-3803

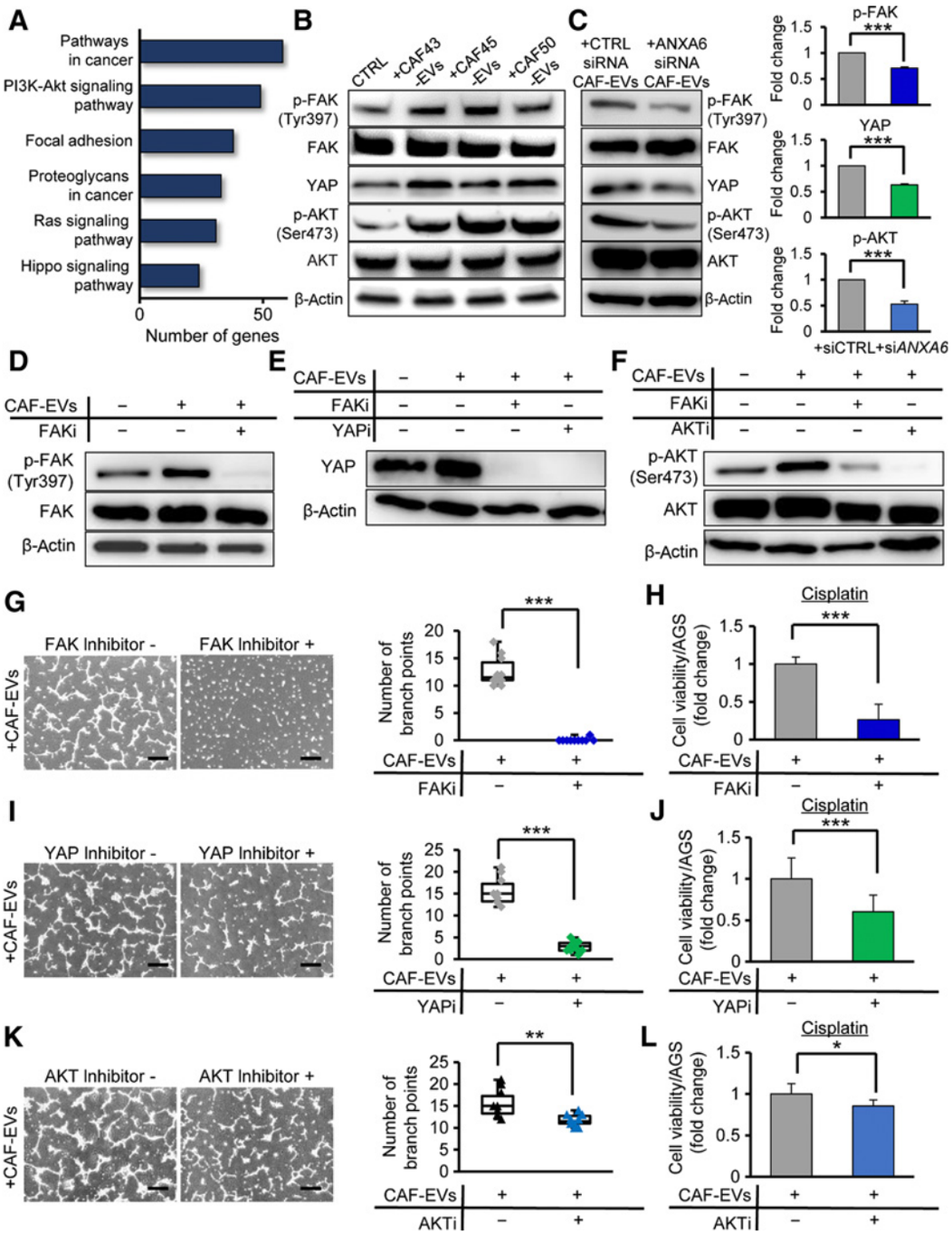

Figure 6.

FAK and YAP inhibitors reduce tubular network formation/drug resistance of gastric cancer cells enhanced by CAF-EVs in the ECM. **A,** Pathway analysis of RNA sequencing and proteomics data from gastric cancer cells after CAF-CM treatment (RNA sequencing, 3 and 24 hours; proteomics, 24 hours). **B** and **C,** Western blots showing the indicated proteins in gastric cancer cells with/without CAF-EVs (**B**) with siCTRL- or si*ANXA6*-transfected CAF-EVs (**C**). The column graphs show the quantification of p-FAK-to-FAK, YAP-to-β-actin, and p-AKT-to-AKT band intensity ratio, respectively (**C**). **D–F,** Western blots showing p-FAK and total FAK expression in gastric cancer cells treated with/without 10 μmol/L FAK inhibitor and CAF-EVs (**D**), YAP expression in gastric cancer cells treated with/without 10 μmol/L FAK inhibitor/1 μmol/L YAP inhibitor and CAF-EVs (**E**), and p-AKT and AKT expression in gastric cancer cells treated with/without 10 μmol/L FAK inhibitor/2 μmol/L AKT inhibitor and CAF-EVs (**F**). **G,** Morphology and network formation of gastric cancer cells after treatment with CAF-EVs and the FAK inhibitor (10 μmol/L). Scale bars, 500 μm. **H,** Gastric cancer cell viability after treatment with CAF-EVs and the FAK inhibitor (10 μmol/L). **I,** Morphology and network formation of gastric cancer cells after treatment with CAF-EVs and the YAP inhibitor (1 μmol/L). Scale bars, 500 μm. **J,** Gastric cancer cell viability after treatment with CAF-EVs and the YAP inhibitor (1 μmol/L). **K,** Morphology and network formation of gastric cancer cells after treatment with CAF-EVs and the AKT inhibitor (2 μmol/L). Scale bars, 500 μm. **L,** Gastric cancer cell viability after treatment with CAF-EVs and the AKT inhibitor (2 μmol/L). *, $P < 0.05$; **, $P < 0.01$; ***, $P < 0.001$.

Published OnlineFirst June 30, 2020; DOI: 10.1158/0008-5472.CAN-19-3803

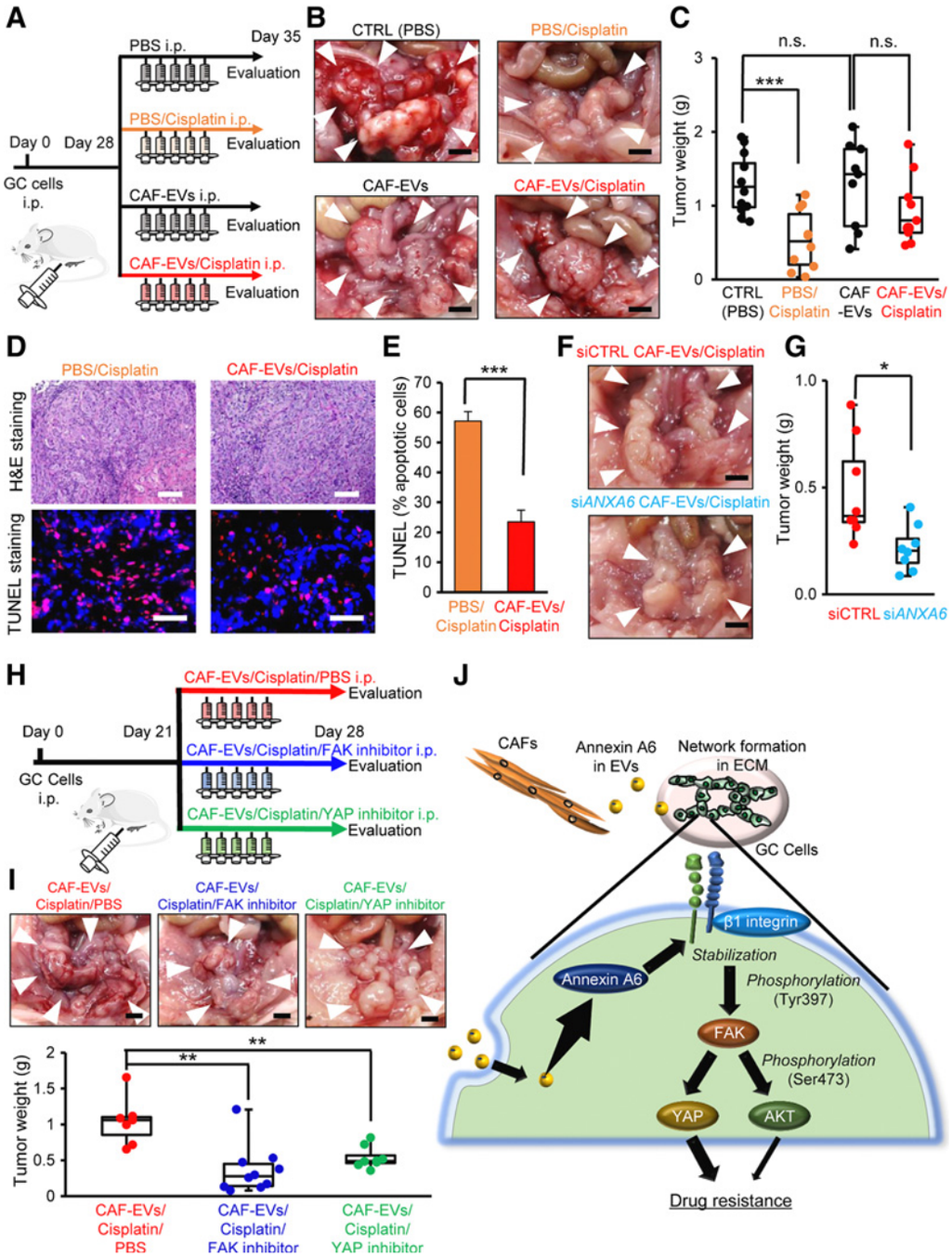

Figure 7.

FAK and YAP inhibitors markedly attenuate drug resistance enhanced by CAF-EVs in a mouse model of peritoneal metastasis. **A–C,** NUGC3 orthotopic xenografts were injected intraperitoneally into mice. After 28 days, the mice were injected intraperitoneally with PBS ($n = 12$), PBS/cisplatin ($n = 10$), CAF-EVs ($n = 9$), and CAF-EVs/cisplatin ($n = 9$) for 5 days. Two days after injection, the mice were euthanized, and the tumors were dissected and weighed (**A**). **B,** Images showing peritoneal metastasis. Scale bars, 5 mm. **C,** Tumor weights. **D** and **E,** Representative hematoxylin and eosin (H&E) and TUNEL staining of peritoneal tumors from mice (**D**) and quantification of TUNEL-positive cells (**E**). Scale bars, hematoxylin and eosin, 100 μm; TUNEL, 50 μm. **F** and **G**, NUGC3 orthotopic xenografts were injected intraperitoneally in mice. After 21 days, siCTRL-transfected CAF-EVs/cisplatin ($n = 8$) and siANXA6-transfected CAF-EVs/cisplatin ($n = 8$) were injected intraperitoneally for 5 days. Two days after injection, the mice were euthanized, and their tumors were dissected and weighed. **F,** Images showing peritoneal metastasis. Scale bars, 5 mm. **G,** Tumor weights. **H** and **I,** NUGC3 orthotopic xenografts were injected intraperitoneally in mice. **H,** After 21 days, CAF-EVs/cisplatin/PBS ($n = 7$), CAF-EVs/cisplatin/FAK inhibitor ($n = 10$), and CAF-EVs/cisplatin/YAP inhibitor ($n = 9$) were injected intraperitoneally for 5 days. Two days after injection, the mice were euthanized, and their tumors were dissected and weighed. **I,** Images showing peritoneal metastasis and tumor weights. Scale bars, 5 mm. **J,** Proposed model of the relationship between CAFs and gastric cancer cells in the ECM. Arrowheads, peritoneal tumors. n.s., not significant; *, $P < 0.05$; **, $P < 0.01$; ***, $P < 0.001$.

Published OnlineFirst June 30, 2020; DOI: 10.1158/0008-5472.CAN-19-3803

stroma is a novel target for combination therapy with currently available anticancer drugs.

Disclosure of Potential Conflicts of Interest

No potential conflicts of interest were disclosed.

Authors' Contributions

T. Uchihara: Conceptualization, resources, data curation, software, formal analysis, validation, investigation, visualization, methodology, writing-original draft, writing-review and editing. **K. Miyake:** Resources, investigation, methodology. **A. Yonemura:** Resources, formal analysis, methodology. **Y. Komohara:** Resources, investigation, visualization, methodology. **R. Itoyama:** Resources, methodology. **M. Koiwa:** Formal analysis, validation. **T. Yasuda:** Formal analysis, validation. **K. Arima:** Resources. **K. Harada:** Resources. **K. Eto:** Resources. **H. Hayashi:** Resources. **M. Iwatsuki:** Resources. **S. Iwagami:** Resources. **Y. Baba:** Resources. **N. Yoshida:** Resources. **M. Yashiro:** Resources, supervision. **M. Masuda:** Formal analysis, supervision. **J. Ajani:** Supervision, writing-review and editing. **P. Tan:** Supervision, writing-review and editing. **H. Baba:** Conceptualization, supervision, writing-original draft, writing-review and editing. **T. Ishimoto:** Conceptualization, data curation, formal analysis, supervision, funding acquisition, validation, investigation, visualization, methodology, writing-original draft, project administration, writing-review and editing.

Acknowledgments

We thank Y. Takahashi (Department of Cell Pathology, Kumamoto University) for her help with the electron microscopy and S. Usuki and N. Tani (Liaison Laboratory Research Promotion Center, IMEG, Kumamoto University) for their help with the RNA sequencing and LC/MS-MS analyses. This work was supported by the Japan Society for the Promotion of Science (JSPS, KAKENHI grant nos. 16H06257, 18K08543, 19K16720, and 20H03531), by the Princess Takamatsu Cancer Research Fund (grant no. 18-25001), by the Takeda Science Foundation, by the NOVARTIS Foundation for the Promotion of Science, by the Foundation for Promotion of Cancer Research, and by the Inter-University Research Network for Trans-Omics Medicine program at the Institute of Molecular Embryology and Genetics at Kumamoto University.

The costs of publication of this article were defrayed in part by the payment of page charges. This article must therefore be hereby marked *advertisement* in accordance with 18 U.S.C. Section 1734 solely to indicate this fact.

Received December 4, 2019; revised April 10, 2020; accepted June 25, 2020; published first June 30, 2020.

References

1. Bray F, Ferlay J, Soerjomataram I, Siegel RL, Torre LA, Jemal A. Global cancer statistics 2018: GLOBOCAN estimates of incidence and mortality worldwide for 36 cancers in 185 countries. CA Cancer J Clin 2018;68:394–424.
2. Kang YK, Boku N, Satoh T, Ryu MH, Chao Y, Kato K, et al. Nivolumab in patients with advanced gastric or gastro-oesophageal junction cancer refractory to, or intolerant of, at least two previous chemotherapy regimens (ONO-4538-12, ATTRACTION-2): a randomised, double-blind, placebo-controlled, phase 3 trial. Lancet 2017;390:2461–71.
3. Hazlehurst LA, Landowski TH, Dalton WS. Role of the tumor microenvironment in mediating *de novo* resistance to drugs and physiological mediators of cell death. Oncogene 2003;22:7396–402.
4. Quail DF, Joyce JA. Microenvironmental regulation of tumor progression and metastasis. Nat Med 2013;19:1423–37.
5. Ruffell B, Coussens LM. Macrophages and therapeutic resistance in cancer. Cancer Cell 2015;27:462–72.
6. Wu Y, Grabsch H, Ivanova T, Tan IB, Murray J, Ooi CH, et al. Comprehensive genomic meta-analysis identifies intra-tumoural stroma as a predictor of survival in patients with gastric cancer. Gut 2013;62:1100–11.
7. Kemi N, Eskuri M, Herva A, Leppanen J, Huhta H, Helminen O, et al. Tumour-stroma ratio and prognosis in gastric adenocarcinoma. Br J Cancer 2018;119:435–9.
8. Lee D, Ham IH, Son SY, Han SU, Kim YB, Hur H. Intratumor stromal proportion predicts aggressive phenotype of gastric signet ring cell carcinomas. Gastric Cancer 2017;20:591–601.
9. Ishimoto T, Miyake K, Nandi T, Yashiro M, Onishi N, Huang KK, et al. Activation of transforming growth factor beta 1 signaling in gastric cancer-associated fibroblasts increases their motility, via expression of rhomboid 5 homolog 2, and ability to induce invasiveness of gastric cancer cells. Gastroenterology 2017;153:191–204.e16.
10. Costa A, Kieffer Y, Scholer-Dahirel A, Pelon F, Bourachot B, Cardon M, et al. Fibroblast heterogeneity and immunosuppressive environment in human breast cancer. Cancer Cell 2018;33:463–79.
11. Bu L, Baba H, Yoshida N, Miyake K, Yasuda T, Uchihara T, et al. Biological heterogeneity and versatility of cancer-associated fibroblasts in the tumor microenvironment. Oncogene 2019;38:4887–901.
12. Izumi D, Ishimoto T, Miyake K, Sugihara H, Eto K, Sawayama H, et al. CXCL12/CXCR4 activation by cancer-associated fibroblasts promotes integrin beta1 clustering and invasiveness in gastric cancer. Int J Cancer 2016;138:1207–19.
13. Maeda M, Takeshima H, Iida N, Hattori N, Yamashita S, Moro H, et al. Cancer cell niche factors secreted from cancer-associated fibroblast by loss of H3K27me3. Gut 2020;69:243–51.
14. Au Yeung CL, Co NN, Tsuruga T, Yeung TL, Kwan SY, Leung CS, et al. Exosomal transfer of stroma-derived miR21 confers paclitaxel resistance in ovarian cancer cells through targeting APAF1. Nat Commun 2016;7:11150.
15. Qin X, Guo H, Wang X, Zhu X, Yan M, Wang X, et al. Exosomal miR-196a derived from cancer-associated fibroblasts confers cisplatin resistance in head and neck cancer through targeting CDKN1B and ING5. Genome Biol 2019;20:12.
16. Fuyuhiro Y, Yashiro M, Noda S, Kashiwagi S, Matsuoka J, Doi Y, et al. Upregulation of cancer-associated myofibroblasts by TGF-beta from scirrhous gastric carcinoma cells. Br J Cancer 2011;105:996–1001.
17. Yamada T, Ohta K, Motooka Y, Fujino K, Kudoh S, Tenjin Y, et al. Significance of Tsukushi in lung cancer. Lung Cancer 2019;131:104–11.
18. Sakurai Y, Uraguchi T, Imazu H, Hasegawa S, Matsubara T, Ochiai M, et al. Changes in thymidylate synthase and its inhibition rate and changes in dihydropyrimidine dehydrogenase after the administration of 5-fluorouracil with cisplatin to nude mice with gastric cancer xenograft SC-1-NU. Gastric Cancer 2004;7:110–6.
19. Hochwald SN, Nyberg C, Zheng M, Zheng D, Wood C, Massoll NA, et al. A novel small molecule inhibitor of FAK decreases growth of human pancreatic cancer. Cell Cycle 2009;8:2435–43.
20. Liu-Chittenden Y, Huang B, Shim JS, Chen Q, Lee SJ, Anders RA, et al. Genetic and pharmacological disruption of the TEAD-YAP complex suppresses the oncogenic activity of YAP. Genes Dev 2012;26:1300–5.
21. Karroum A, Mirshahi P, Benabbou N, Faussat AM, Soria J, Therwath A, et al. Matrix metalloproteinase-9 is required for tubular network formation and migration of resistant breast cancer cells MCF-7 through PKC and ERK1/2 signalling pathways. Cancer Lett 2010;295:242–51.
22. Hu B, Wang Q, Wang YA, Hua S, Sauve CG, Ong D, et al. Epigenetic activation of WNT5A drives glioblastoma stem cell differentiation and invasive growth. Cell 2016;167:1281–95.
23. Donaldson KL, Goolsby GL, Wahl AF. Cytotoxicity of the anticancer agents cisplatin and taxol during cell proliferation and the cell cycle. Int J Cancer 1994;57:847–55.
24. Meldolesi J. Exosomes and ectosomes in intercellular communication. Curr Biol 2018;28:R435–44.
25. Colombo M, Raposo G, Thery C. Biogenesis, secretion, and intercellular interactions of exosomes and other extracellular vesicles. Annu Rev Cell Dev Biol 2014;30:255–89.
26. Naito Y, Yamamoto Y, Sakamoto N, Shimomura I, Kogure A, Kumazaki M, et al. Cancer extracellular vesicles contribute to stromal heterogeneity by inducing chemokines in cancer-associated fibroblasts. Oncogene 2019;38:5566–79.
27. Leca J, Martinez S, Lac S, Nigri J, Secq V, Rubis M, et al. Cancer-associated fibroblast-derived annexin A6+ extracellular vesicles support pancreatic cancer aggressiveness. J Clin Invest 2016;126:4140–56.
28. Desgrosellier JS, Cheresh DA. Integrins in cancer: biological implications and therapeutic opportunities. Nat Rev Cancer 2010;10:9–22.
29. Barczyk M, Carracedo S, Gullberg D. Integrins. Cell Tissue Res 2010;339:269–80.

30. Zeltz C, Primac I, Erusappan P, Alam J, Noel A, Gullberg D. Cancer-associated fibroblasts in desmoplastic tumors: emerging role of integrins. Semin Cancer Biol 2020;62:166–81.
31. Xia H, Nho RS, Kahm J, Kleidon J, Henke CA. Focal adhesion kinase is upstream of phosphatidylinositol 3-kinase/Akt in regulating fibroblast survival in response to contraction of type I collagen matrices via a beta 1 integrin viability signaling pathway. J Biol Chem 2004;279:33024–34.
32. Nardone G, Oliver-De La Cruz J, Vrbsky J, Martini C, Pribyl J, Skladal P, et al. YAP regulates cell mechanics by controlling focal adhesion assembly. Nat Commun 2017;8:15321.
33. Sabra H, Brunner M, Mandati V, Wehrle-Haller B, Lallemand D, Ribba AS, et al. beta1 integrin-dependent Rac/group I PAK signaling mediates YAP activation of Yes-associated protein 1 (YAP1) via NF2/merlin. J Biol Chem 2017;292:19179–97.
34. Tan P, Yeoh KG. Genetics and molecular pathogenesis of gastric adenocarcinoma. Gastroenterology 2015;149:1153–62.
35. Tkach M, Thery C. Communication by extracellular vesicles: where we are and where we need to go. Cell 2016;164:1226–32.
36. Fujita Y, Yoshioka Y, Ochiya T. Extracellular vesicle transfer of cancer pathogenic components. Cancer Sci 2016;107:385–90.
37. Kosaka N, Yoshioka Y, Fujita Y, Ochiya T. Versatile roles of extracellular vesicles in cancer. J Clin Invest 2016;126:1163–72.
38. Gyorgy B, Szabo TG, Pasztoi M, Pal Z, Misjak P, Aradi B, et al. Membrane vesicles, current state-of-the-art: emerging role of extracellular vesicles. Cell Mol Life Sci 2011;68:2667–88.
39. Smith DL, Evans CA, Pierce A, Gaskell SJ, Whetton AD. Changes in the proteome associated with the action of Bcr-Abl tyrosine kinase are not related to transcriptional regulation. Mol Cell Proteomics 2002;1:876–84.
40. Grewal T, Evans R, Rentero C, Tebar F, Cubells L, de Diego I, et al. Annexin A6 stimulates the membrane recruitment of p120GAP to modulate Ras and Raf-1 activity. Oncogene 2005;24:5809–20.
41. Garcia-Melero A, Reverter M, Hoque M, Meneses-Salas E, Koese M, Conway JR, et al. Annexin A6 and late endosomal cholesterol modulate integrin recycling and cell migration. J Biol Chem 2016;291:1320–35.
42. Grewal T, Hoque M, Conway JRW, Reverter M, Wahba M, Beevi SS, et al. Annexin A6-A multifunctional scaffold in cell motility. Cell Adh Migr 2017;11:288–304.
43. Koese M, Rentero C, Kota BP, Hoque M, Cairns R, Wood P, et al. Annexin A6 is a scaffold for PKCalpha to promote EGFR inactivation. Oncogene 2013;32:2858–72.
44. Koumangoye RB, Nangami GN, Thompson PD, Agboto VK, Ochieng J, Sakwe AM. Reduced annexin A6 expression promotes the degradation of activated epidermal growth factor receptor and sensitizes invasive breast cancer cells to EGFR-targeted tyrosine kinase inhibitors. Mol Cancer 2013;12:167.
45. Rankin CR, Hilgarth RS, Leoni G, Kwon M, Den Beste KA, Parkos CA, et al. Annexin A2 regulates beta1 integrin internalization and intestinal epithelial cell migration. J Biol Chem 2013;288:15229–39.
46. Harvey KF, Zhang X, Thomas DM. The Hippo pathway and human cancer. Nat Rev Cancer 2013;13:246–57.
47. Zhao Y, Yang X. The Hippo pathway in chemotherapeutic drug resistance. Int J Cancer 2015;137:2767–73.
48. Feng X, Arang N, Rigiracciolo DC, Lee JS, Yeerna H, Wang Z, et al. A platform of synthetic lethal gene interaction networks reveals that the GNAQ uveal melanoma oncogene controls the hippo pathway through FAK. Cancer Cell 2019;35:457–72.

Published OnlineFirst June 30, 2020; DOI: 10.1158/0008-5472.CAN-19-3803

Cancer Research
The Journal of Cancer Research (1916–1930) | The American Journal of Cancer (1931–1940)

AACR American Association for Cancer Research

Extracellular Vesicles from Cancer-Associated Fibroblasts Containing Annexin A6 Induces FAK-YAP Activation by Stabilizing β1 Integrin, Enhancing Drug Resistance

Tomoyuki Uchihara, Keisuke Miyake, Atsuko Yonemura, et al.

Cancer Res 2020;80:3222-3235. Published OnlineFirst June 30, 2020.

Supplementary Fig. 1

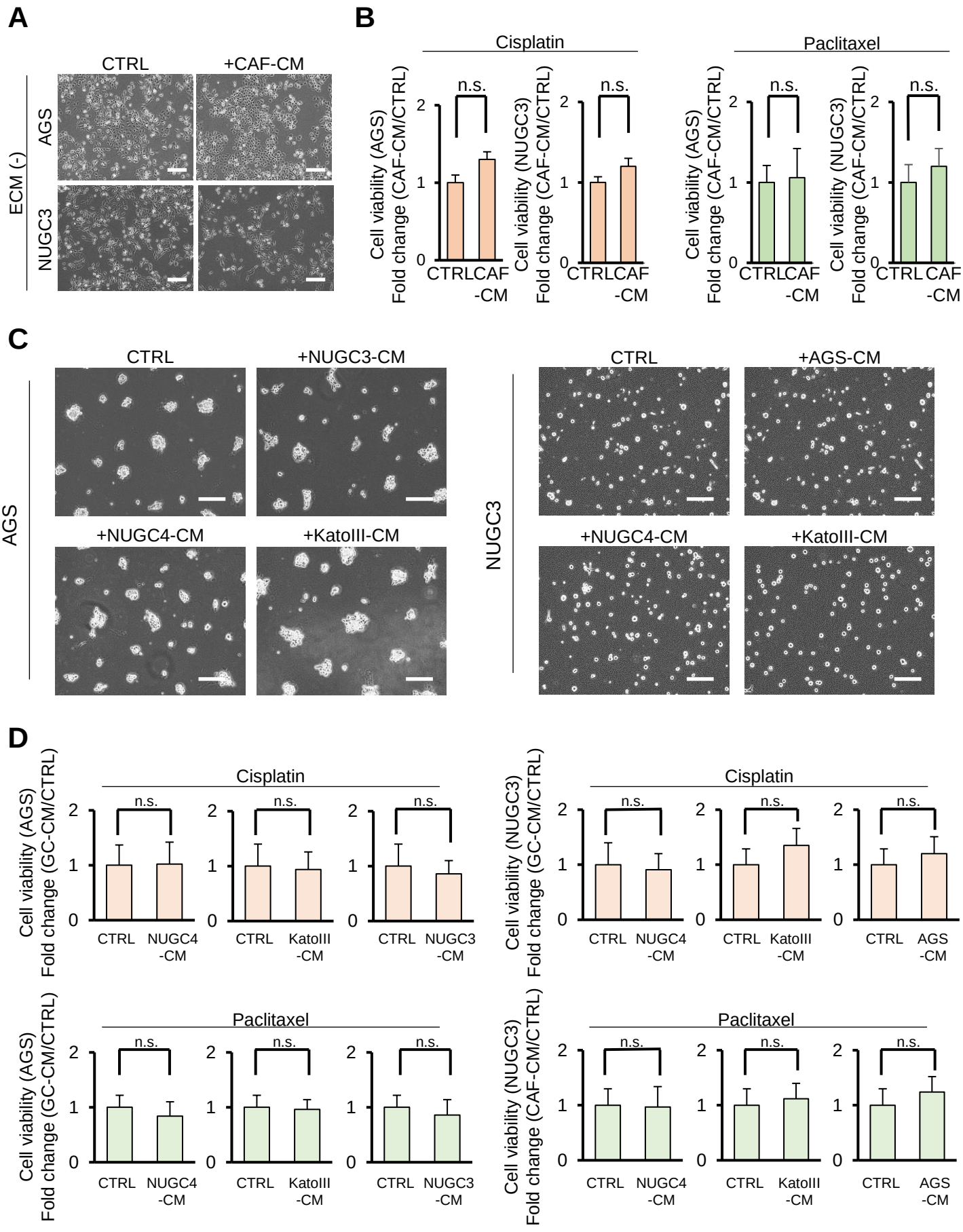

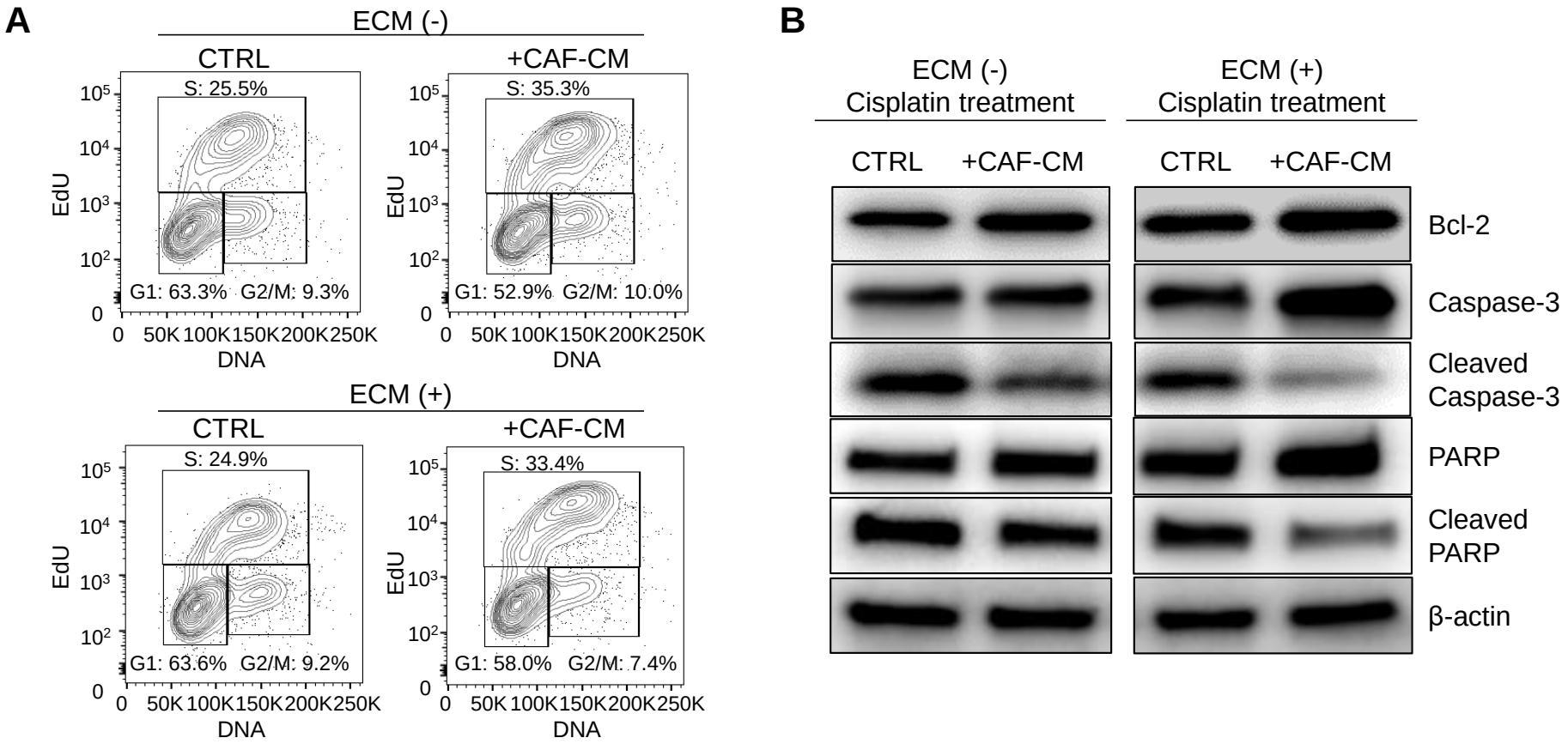

Supplementary Fig. 2

Supplementary Fig. 3

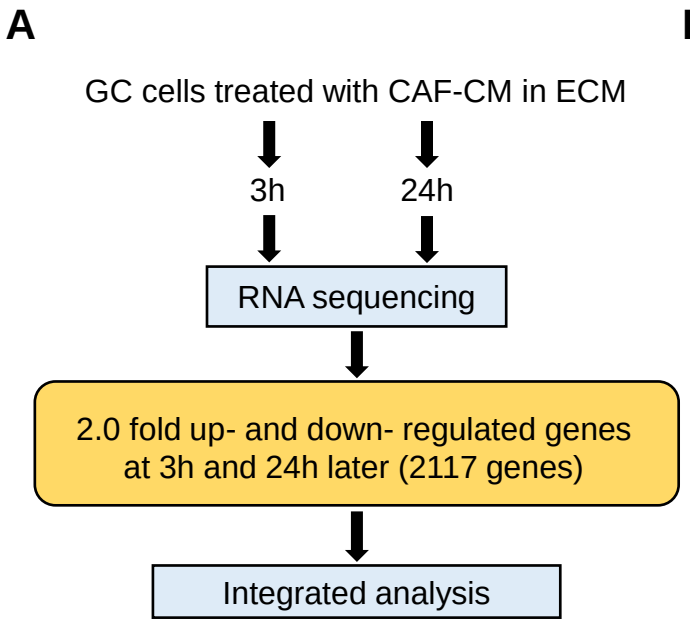

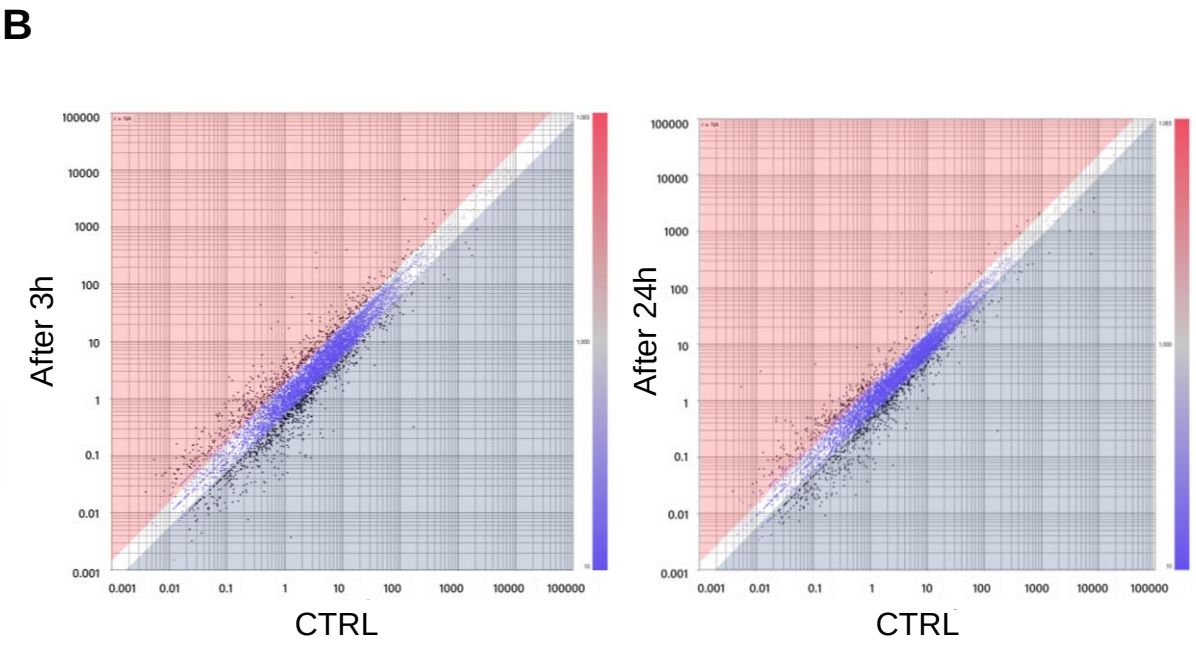

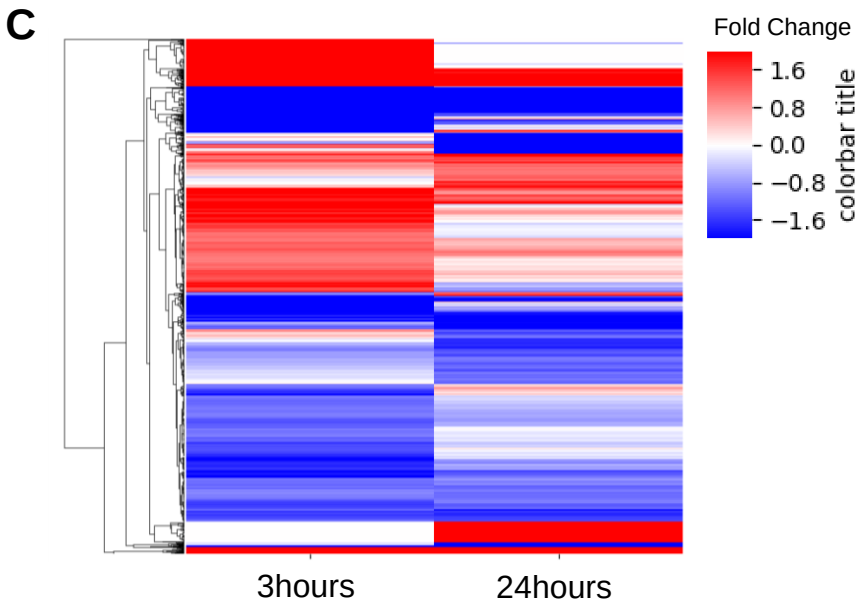

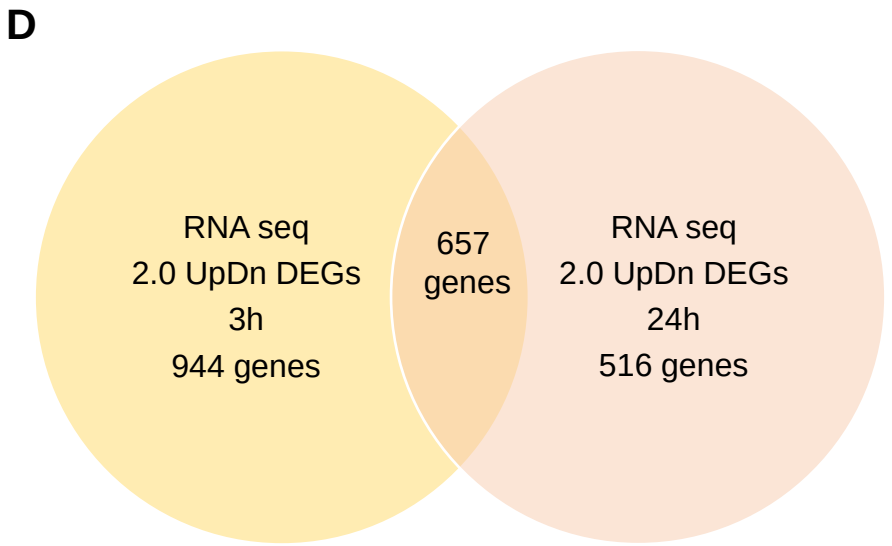

Supplementary Fig. 4

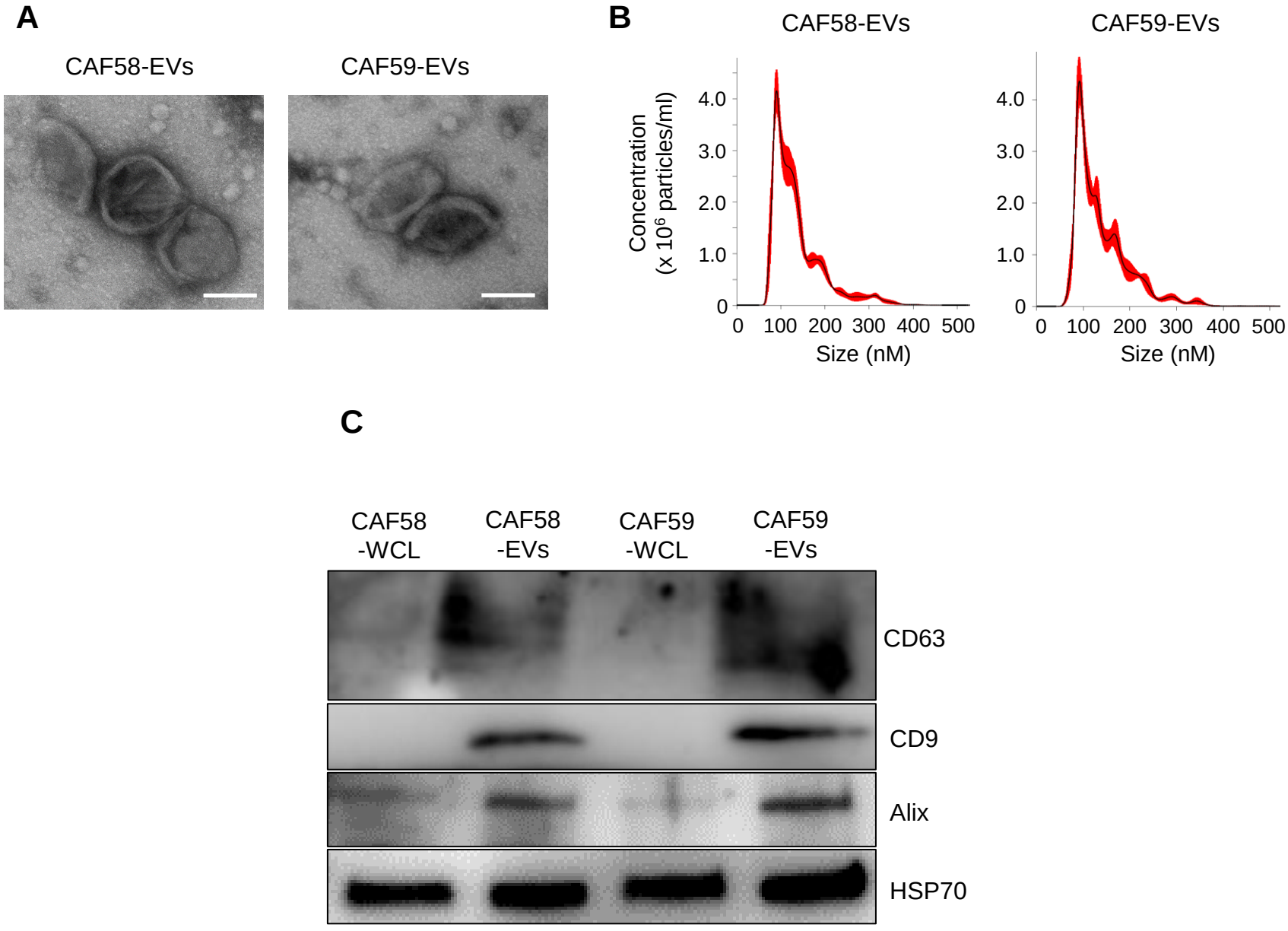

Supplementary Fig. 5

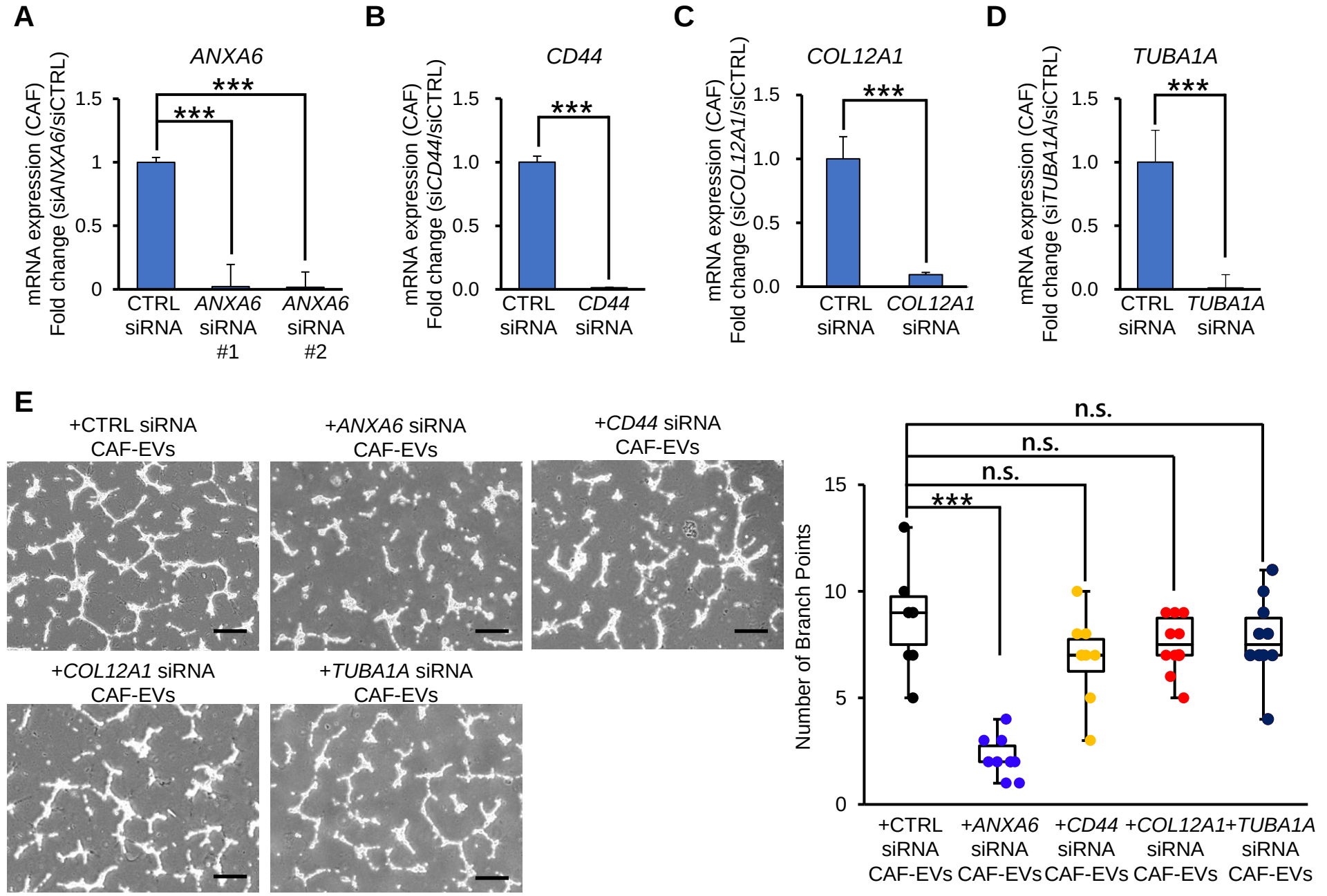

A

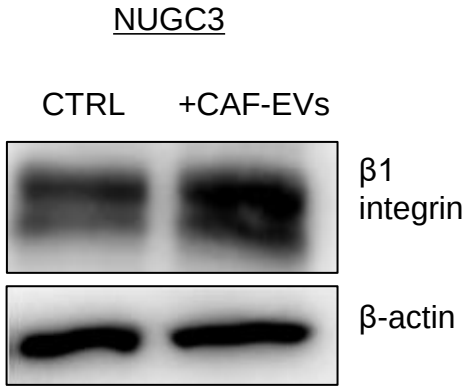

B

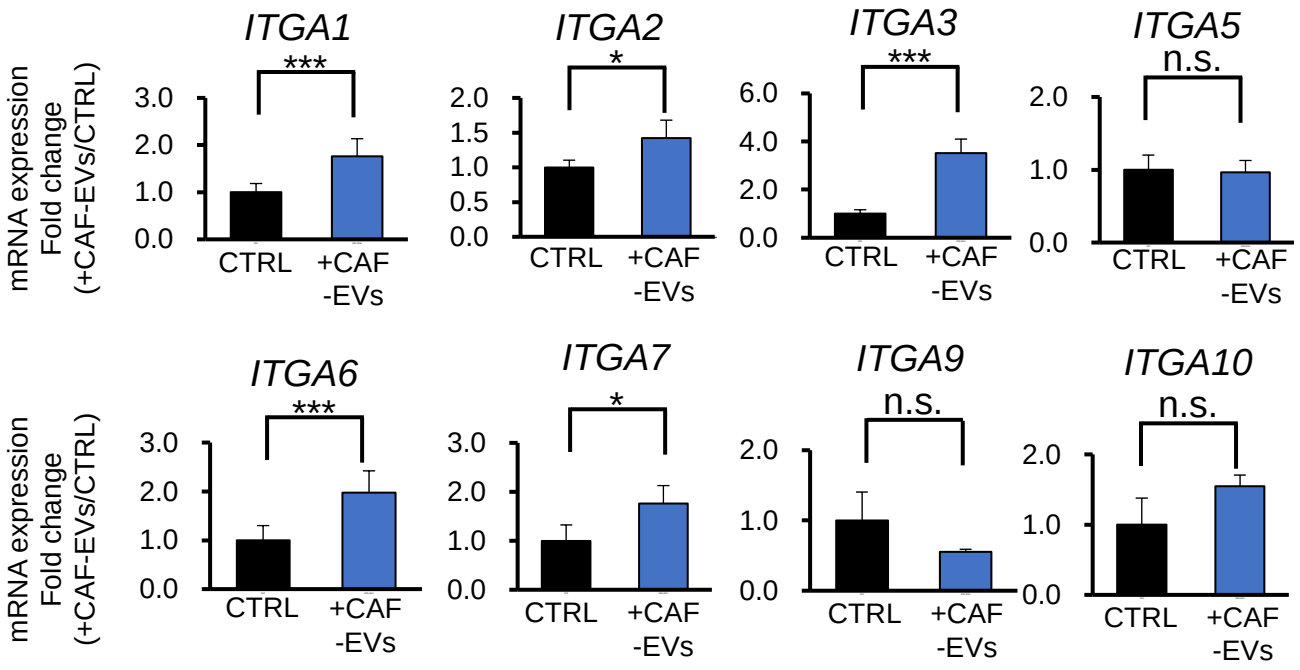

Supplementary Fig. 6

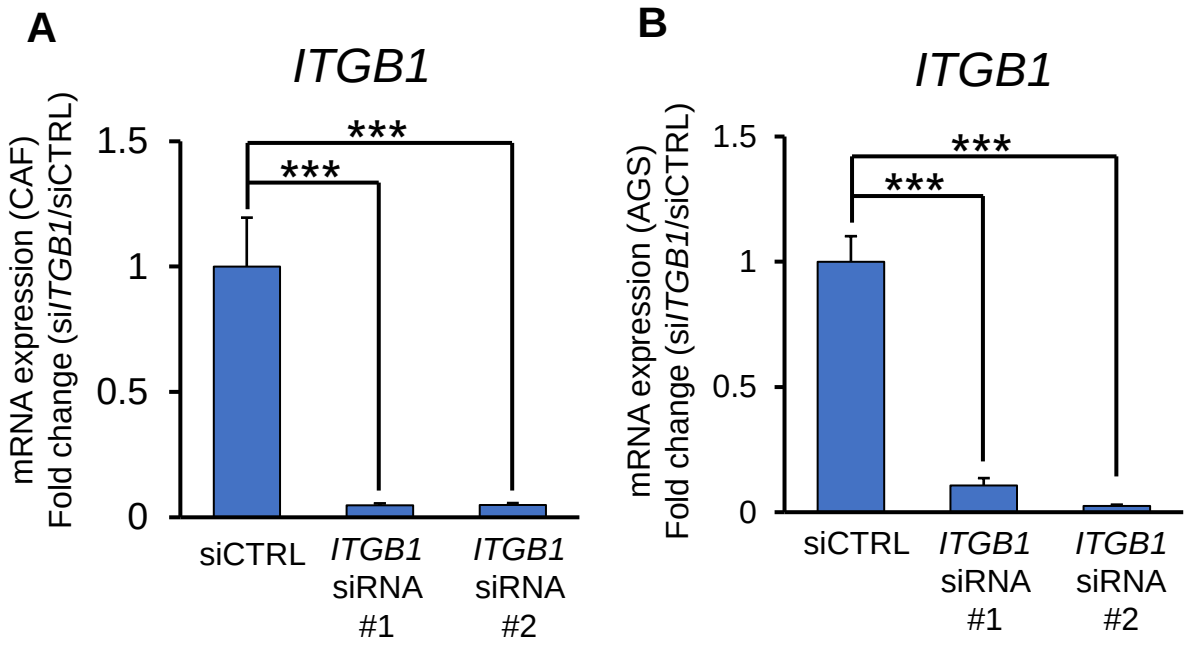

Supplementary Fig. 7

Supplementary Fig. 8

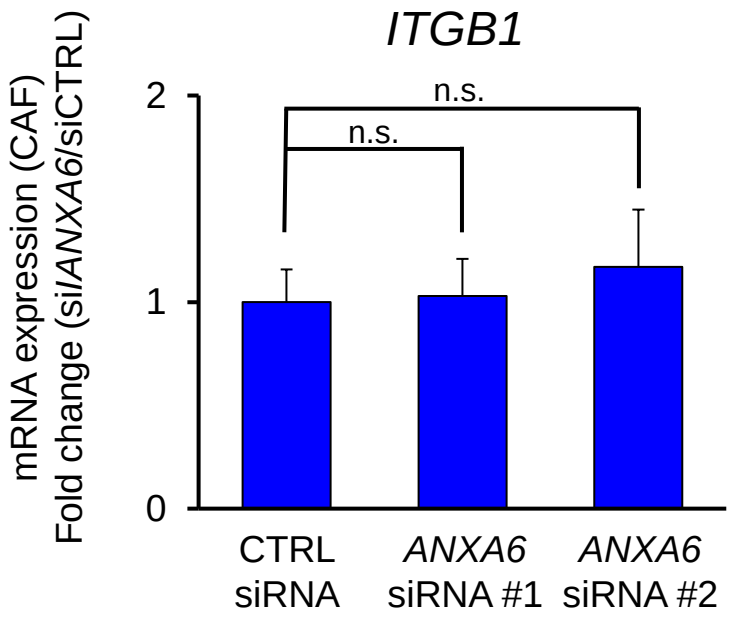

Supplementary Fig. 9

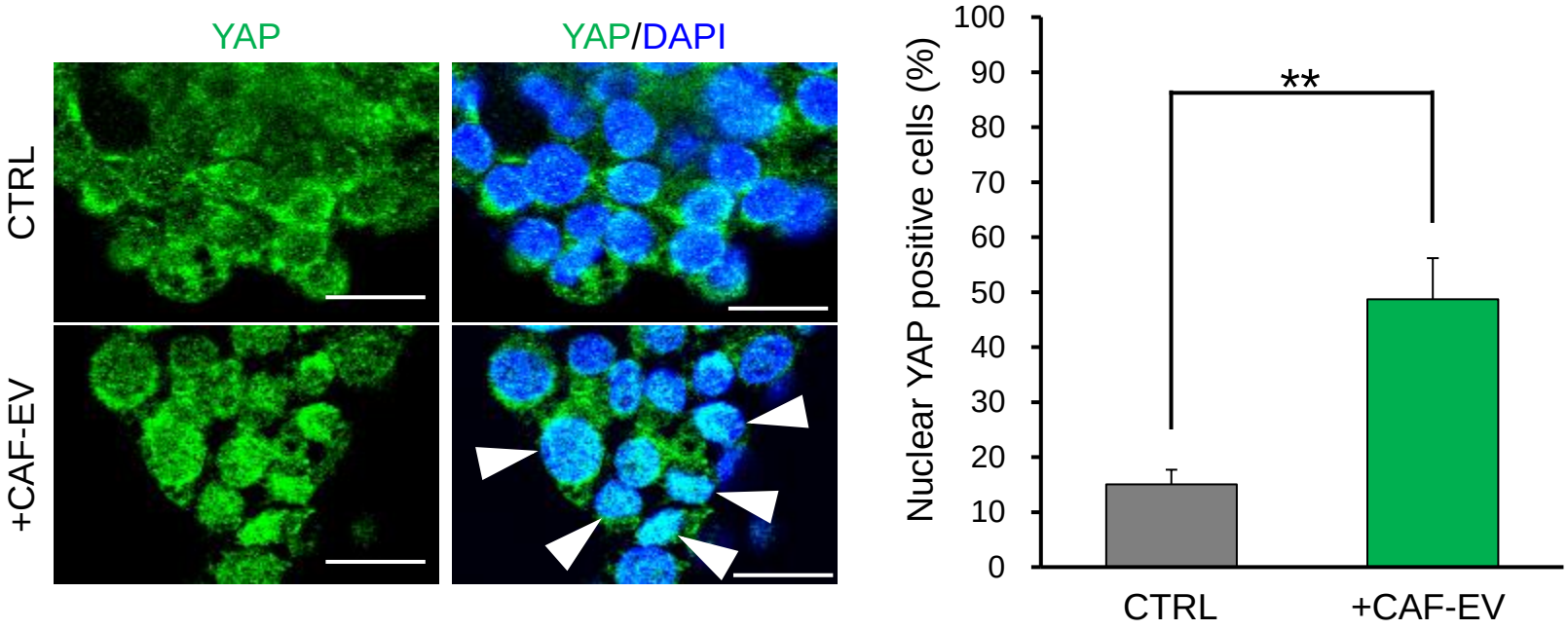

Supplementary Fig. 10